Positron-emitting radionuclides for applications, with special emphasis on their production methodologies for medical use

S. M. Qaim, B. Scholten*, I. Spahn, B. Neumaier

Institut für Neurowissenschaften und Medizin, INM-5: Nuklearchemie, Forschungszentrum Jülich GmbH, 52425 Jülich, Germany

Abstract

A survey of the positron-emitting radionuclides over the whole mass range of the Periodic Table of Elements was carried out. As already known, positrons are preferably emitted from light mass neutron deficient radionuclides. Their emission from heavier mass nuclides is rather rare. The applications of positron annihilation in three areas, namely materials research, plant physiology and medical diagnosis, are reported. The methods of production of positron emitters are discussed, with emphasis on radionuclides presently attracting more attention in theranostics and multimodal imaging. Some future perspectives of radionuclide development technologies are considered.

Keywords: Positron-emitting radionuclide for application, materials research, plant physiology, positron emission tomography, theranostics, multimodal imaging.

*Author for correspondence. E-mail: b.scholten@fz-juelich.de

1. Introduction

Radioactivity is a phenomenon which involves transformation of an unstable nuclide to a more stable nuclide through emission of radiation. Of particular interest in this context is the average binding energy per nucleon ($\overline{E}_B$) of the two nuclides concerned, the transformation always occurring to the nuclide with higher binding energy per nucleon. Since the $\overline{E}_B$ values of nuclides are different in different mass regions of the Periodic Table of Elements, the transformation processes show considerable variations. The unstable nuclides in the heavy mass region, for example, tend to attain stability relatively fast by emitting an α-particle, where the charge Z of the nuclide decreases by 2 units, or even by spontaneous fission, where the nucleus breaks down into two unequal parts. In the light and medium mass regions, on the other hand, nuclear transformations take place mostly in small steps, i.e. by change in Z of the nuclide by one unit. In transformation of a neutron excess radionuclide an electron is emitted which is called a β^- particle. In a neutron deficient radionuclide, on the other hand, either direct capture of an atomic electron occurs (EC) or emission of a positively-charged electron, called a positron (β^+), takes place. The β^+ emission is specifically prevalent in the region of very light mass nuclei ($A < 20$), which is very important in life sciences. With increasing masses of neutron deficient nuclides, EC and β^+ emission processes start competing and the contribution of EC increases. In the mass region around 70, for example, the contribution of EC becomes significant, and for nuclei with A=130, e.g. the neutron deficient radionuclides of rare earth elements, it becomes the dominant decay mode. Furthermore, besides the primary radiation, some secondary radiation emissions like γ-rays, X-rays, Auger and conversion electrons, etc. also gain significance. All those emitted radiations find today applications in internal nuclear medicine in one form or the other, covering both diagnosis and therapy [cf. 1]. The utilization of some of those radiation types is discussed in a few other contributions in this special issue. This article deals with the specific case of positron-emitting radionuclides. Their occurrence, applications and production methodologies are discussed. A list of the positron-emitting radionuclides, which have found some application, scattered over the Periodic Table of Elements is given in Table 1. It is an extended version of the data given in Ref. [2]. Many more short-lived positron emitters exist beyond mass 75, but their utility is not proven. The decay data were taken from Ref. [3], except for a few cases where own measured data are given [4-6]. It is obvious that most of the positron emitters are found in the light mass region whereas their occurence is rather rare in the heavy mass region.

2. Characteristics of the positron

The positron is an antiparticle of the electron. In fact it was the first antiparticle discovered [7]. Thus, it has the same properties as the electron (mass, spin) but its charge is +1 instead of -1. Also the energy spectrum of the positron is similar to that of the electron because in each case part of the energy is transferred to the concurrently emitted neutrino. In general, a free positron cannot exist for a long time except in vacuum. After emission from a radionuclide, the positron first loses energy through scattering in the surrounding material until it is moderated to thermal energy. Thereafter it collides with an electron and gets annihilated converting the mass of the two particles into energy. In some special cases the positron forms a transient pair with an electron called a positronium (Ps) which has a very short life-time and is annihilated with a slight delay. The mode of annihilation depends on the spin orientations of the two collision partners. Annihilation in singlet state (spins in opposite direction) gives 2 annihilation quanta; that in the triplet state (spins parallel) leads to 3 annihilation quanta. In general, two photons emission is most probable (> 99.7 %) [8], each photon having an energy of 511 keV. The two photons are correlated by 180°. A representation of the annihilation process is given in Fig. 1.

The resulting three important characteristics of the positron annihilation process are:

a) the path length covered by the positron before thermalisation,
b) the life-time of the positron before annihilation,
c) the coincident nature of the two γ-photons.

3. Brief overview of applications of positron annihilation

The three characteristics described above have great implications in solid state materials research, plant physiology and medical diagnostic imaging via positron emission tomography (PET). A brief discussion is given below.

3.1. Materials research

The path length of the positron before thermalisation is dependent on the energy of the positron and the medium in which the positron is embedded. A reconstruction of the transport process of the positron thus delivers information on some properties of the absorbing material. Positrons tend to accumulate in vacancies in metal lattices (“metal defects”), i.e. in the regions of low electron densities. The main applications of this phenomenon are therefore reflected in studies dealing with the influence of annealing on radiation damage in metals, in investigations on effect of temperature and pressure on vacancy concentrations in pure metals, etc.

The life-time of the positron is strongly affected by the surrounding material. In a conducting metal it could be very short (10^{-12} s) but in semi-conducting or organic material it is longer (10^{-7} s) due to formation of a positronium. For example, the probability of positronium formation in H_2O was estimated to be about 36 % and in benzene about 57 %. In general, the life-time of the positronium depends on the electron density in the material and, therefore, a study of interaction of positrons with the material leads to chemical information on the surrounding medium.

Over the years the positron annihilation spectroscopy (PAS; positron annihilation life-time spectroscopy PALS) has been developed to a very sophisticated technique for characterisation of surfaces of topological insulator materials and studies on material defects, partly alone, but also in combination with other techniques, like Mössbauer spectroscopy, Doppler broadening spectroscopy, etc. (for recent reviews cf. [9-11]). The positron annihilation spectroscopy is based on measurement of the time difference between the emission of the positron and the registration of the annihilation γ-rays. The start signal, i.e. the emission of the positron from a radionuclide, is generally registered by measurement of a γ-ray emitted by the same radionuclide in coincidence with the positron. The measurements lead to the determination of the life-time of the positron in the material, wherefrom the electron density in the material is deduced. The investigation thus requires a special radionuclide, i.e. a radionuclide which emits, besides the positron, also a suitable γ-ray in coincidence with the positron. The most commonly used radionuclide is ^{22}Na ($T_{½}$ = 2.6 a). In its decay a γ-ray of energy 1274.5 keV follows the emission of the positron. There are a few other useful or potentially useful radionuclides as well, e.g. ^{44m}Sc ($T_{½}$ = 2.44 d), ^{48}V ($T_{½}$ = 15.9 d), ^{68}Ge ($T_{½}$ = 270.8 d) in equilibrium with ^{68}Ga ($T_{½}$ = 1.1 h), etc. The production aspects of some of those radionuclides are considered in detail later in this article.

The use of positrons in materials research follows in four different ways:

i) by placing a small drop of the source activity (typically 1 MBq) between two thin metal or polymer foils [cf. 11],

ii) by implanting the positron emitter in a thin metal foil which then acts as the source [cf. 12],

iii) by using spin-polarized slow positron beams, e.g. from ^{18}F, ^{22}Na, ^{68}Ge, etc. [13, 14], generated in a specially developed apparatus,

iv) by creating a positron through pair production via the interaction of high-energy photons with a converter. The photons are obtained from a high energy electron linear accelerator (LINAC). Such accelerators are commercially available today.

The first three techniques making use of positron-emitting radionuclides are more relevant to this article.

3.2 Plant physiology

A large number of radionuclides have found application in tracer studies related to plant biology, using both *in vivo* and *in vitro* investigations. However, because of the coincident emission of two annihilation quanta in the decay of positron emitters, some special physiological functions in plants are advantageously studied *in vivo* using organic positron emitters and a few metallic positron emitters like ^{48}V ($T_{½}$ = 16.0 d), ^{52}Fe ($T_{½}$ = 8.3 h), etc.. The emphasis, however, lies on organic positron emitters, namely ^{11}C ($T_{½}$ = 20.4 min) and ^{13}N ($T_{½}$ = 10.0 min) and to some extent on ^{15}O ($T_{½}$ = 2.3 min) and ^{18}F ($T_{½}$ = 109.8 min). The investigations are generally related to leaf photosynthesis, including $^{11}CO_2$ fixation, leaf export of ^{11}C-photosynthates, uptake of a carbon-containing compound (labelled with ^{11}C) by the leaf or the stem of a plant, and its disintegration or transport towards the root, etc. Other studies are related to uptake of nitrogen-containing compounds (with ^{13}N as a tracer), e.g. $^{13}NH_3$ by leaves, $[^{13}N]N_2$ by roots, etc. However, due to the short half-lifes of the radionuclides used, their application can be effected only in the vicinity of a production cyclotron. In the last few years, in many cyclotron laboratories such plant physiological studies have been included. However, extensive efforts have been devoted to such investigations at three large research centres, namely Forschungszentrum Jülich (Germany), Brookhaven National Laboratory (USA) and Research Centre Takasaki (Japan), each centre having several cooperative partners. The salient features of those studies are given in a few recent reviews [15-20]. The techniques have reached a great degree of sophistication through a combination of positron emission tomography (PET) with magnetic resonance imaging (MRI) [cf. 15, 16]. On the other hand, efforts are also being intensified to develop real-time radioisotope imaging methods to study living plant activity, both for elements and water, revealing some new aspects of plant physiology (for a review cf. [21]).

3.3 Medical diagnosis *via* positron emission tomography (PET)

This is the most widely expanding field of application of positron-emitting radionuclides. Whereas in materials research the positron and its annihilation time are of primary interest, no matter where the positron comes from, i.e. whether from a radionuclide or from an accelerator, in PET studies (related to both plant physiology and medical diagnosis) the whole radionuclide and its chemical binding are of great importance. The radionuclide is intentionally attached to a molecule to facilitate its movement in the body and its localisation in a given organ under investigation. The positron annihilation time is not of much consequence, but the other two characteristics, namely the path length in the tissue prior to annihilation and the coincident nature of the annihilation quanta are of paramount importance.

Although not many experimental measurements related to positrons and positronium chemistry in tissue have been performed, it is argued theoretically and concluded therefrom that most of the annihilations in tissue result in two γ-ray emission [cf. 22]. Measurement of the two γ-rays in coincidence thus makes the technique quantitative. This is a unique and very advantageous characteristic of the PET methodology. On the other hand, if other γ-rays emitted by the radionuclide lie in the vicinity of the 511 keV photons, some random coincidences may occur. A scattering correction then becomes essential [cf. 23]. In general, therefore, radionuclides with high positron-emission intensity and no or very low γ-ray emission are considered most suitable.

The spatial resolution in PET imaging is limited by the path length (i.e. the range) of the positron prior to its annihilation, which depends on its initial kinetic energy. For example, the maximum β^+ energy of ^{18}F is 0.63 MeV and the average energy about 0.25 MeV. This results in a range distribution with a FWHM of approximately 1.0 mm. In contrast, the maximum β^+energy of ^{76}Br amounts to about 4.0 MeV which results in a range distribution having a FWHM of approximately 6.0 mm. Consequently, the resolution of the PET scan is deteriorated. Therefore, positron-emitting radionuclides with low kinetic energies are preferable.

Most of the PET measurements in diagnostic nuclear medicine deal with fast metabolic processes, which involve use of standard short-lived positron emitters (^{11}C, ^{18}F, ^{68}Ga, etc.)

attached to suitable organic molecules. Such investigations are generally well established and are routinely performed in patient care programmes. However, many slow biological processes cannot be investigated using those radionuclides. For such processes longer lived positron emitters are needed. There are two other emerging applications of PET radionuclides. One entails a combination of PET with magnetic resonance imaging (MRI). Another one makes use of a diagnostic and therapeutic pair of the same element for theranostic approaches.

It is understood that out of all the positron emitters listed in Table 1, only a limited number of them is suitable or potentially suitable for medical applications. The production methods of some important radionuclides are discussed below.

4. Production of positron-emitting radionuclides

The so-called “four basic pillars” of the radionuclide production technology, namely nuclear data, irradiation targetry, chemical processing and quality assurance of the product [cf. 24], have all to be well developed to establish a reliable supply of the positron-emitting radionuclide for routine patient applications. Such a radionuclide is then termed as a “standard positron emitter”. In contrast, novel positron-emitting radionuclides for which development work is still going on or which are not commercially available are called “non-standard positron emitters”. We discuss the production methods of the two types of positron emitters in some detail below.

4.1 Standard positron emitters

Several nuclear reactions have been investigated for the production of positron emitters (for early review cf. [25]). The common methods used today for the production of the seven standard positron emitters, viz. ^{11}C, ^{13}N, ^{15}O, ^{18}F, ^{22}Na, ^{68}Ga and ^{82}Rb are summarized in Table 2. They are all produced directly via charged-particle induced reactions, except for ^{68}Ga and ^{82}Rb, which are made available via generator systems. The parent generator radionuclides, however, are also produced using charged-particle induced reactions. All of them except for ^{22}Na find application in routine patient care studies using PET. The radionuclide ^{22}Na is the major positron emitter used routinely in materials research. The radionuclides ^{11}C and ^{13}N are often employed in plant physiological studies.

The first four radionuclides, often termed as organic positron emitters, are typically produced at a medical cyclotron ($E_p \leq 18$ MeV; $E_d \leq 9$ MeV). The extensive development work carried out in many laboratories was evaluated in early 1990s under a COST Action of the European Union (EU) and the most suitable production methodologies were recommended [26]. Later on, the cross section data were evaluated and standardized under the auspices of the International Atomic Energy Agency (IAEA), and the recommended values are given in Ref. [27]. The electronic version of the file is updated periodically. The calculated yields for all reactions given in Table 2 are based on those data except for the $^{18}O(p,n)^{18}F$ reaction where extensive measurements by Hess et al. [28] were used to calculate the yields. In general, at a medical cyclotron only gas and liquid targets are available, and they are sufficient for the production of the above mentioned four organic positron emitters. Thus ^{11}C, ^{15}O and $[^{18}F]F_2$ are produced using pressurized gas targets, and ^{13}N and $^{18}F^{-}_{(aq)}$ using pressurized water targets. The enrichment of the target material used, the chemical form of the radionuclide produced in the target and the typical batch yields achieved [24, 29] are also listed in Table 2. The production technology of those radionuclides is well established and the standard PET imaging technique is rapidly expanding. The radionuclide ^{18}F has become the positron emitter of paramount importance in PET imaging.

In recent years most of the development work related to the production of the above mentioned organic positron emitters has concentrated on increasing the radionuclidic purity of all radionuclides, the specific activity of ^{11}C, the batch yield of $^{18}F^{-}_{(aq)}$, and the yield and specific activity of $[^{18}F]F_2$. We consider a few features of those development studies.

The activation products formed in the interaction of nitrogen with protons of energy up to 200 MeV were measured. The results up to 20 MeV are relevant to this article and are shown in Fig. 2. The dominating reaction is the $^{14}N(p,\alpha)^{11}C$ process which is commonly used for the production of ^{11}C ($T_{½}$ = 20.4 min). Its cross section data have been standardized (see above). The relatively new data [cf. 30] for the reactions $^{14}N(p,n)^{14}O$ and $^{14}N(p,pn)^{13}N$, leading to the positron emitting undesired radionuclides ^{14}O ($T_{½}$ = 70 s) and ^{13}N ($T_{½}$ = 10.0 min), respectively, make it possible to calculate the radioactive impurities formed during the production of ^{11}C. For the proton energy range within the nitrogen gas target ($E_p = 13 \rightarrow 4$ MeV) it is estimated that the ^{11}C formed will contain about 20 % ^{14}O and 5 % ^{13}N at the end of irradiation. This is very useful information to ensure the final radionuclidic purity of the ^{11}C-labelled compound. Similar studies have been performed in the case of ^{15}O production via the $^{14}N(d,n)$-reaction [cf. 31]. Regarding the specific activity of ^{11}C, special precautions are necessary with respect to gas composition, target construction and chemicals used, since stable ^{12}C is present everywhere. Under optimum conditions $[^{11}C]CO_2$ was obtained in high specific activity up to 610 GBq/µmol [cf. 32]. With regard to the batch yield of ^{18}F, targetry has been advanced at commercial units and up to 400 GBq of $^{18}F^-_{(aq)}$ are produced routinely. These quantities as well as the specific activity of ^{18}F are sufficient for preparation of most of the radiopharmaceuticals via nucleophilic reactions for routine use. However, for preparation of some radiopharmaceuticals, still electrophilic reactions are more favourable. The starting labelling species $[^{18}F]F_2$ was previously obtained via the $^{20}Ne(d,\alpha)$-reaction but both the yield and the specific activity were limited [cf. 33]. A modified route involving the $^{18}O(p,n)^{18}F$ reaction using an enriched gas target and two successive irradiations led to improved results [34, 35]. Under optimized conditions a batch yield of about 25 GBq of $[^{18}F]F_2$ was obtained and its specific activity amounted to about 0.6 TBq/mmol [35]. This specific activity may be sufficient for preparation of a few compounds but, in general, a still higher specific activity is needed. Attempts have therefore also been directed to convert the nucleophilic form of ^{18}F to the electrophilic form. However, hitherto only modest success has been achieved [cf. 37].

For the production of ^{22}Na, the standard positron emitter used in materials research, several nuclear routes were investigated (for an early review, cf. [38]). The cross section data for all those reactions given in the EXFOR file of the IAEA [39] were considered, smooth eye-guided curves were fitted, and the results are given in Fig. 3(A) and (B). They describe the reactions induced by protons and deuterons on Al and Mg, by protons on Ne and by α-particles on F and Al. Among the low-energy reactions (Fig. 3 (A)), the $^{nat}Mg(d,x)^{22}Na$ process has been commonly used. Among the intermediate energy reactions (Fig. 3 (B)), on the other hand, the $^{nat}Mg(p,x)^{22}Na$ and $^{27}Al(p,x)^{22}Na$ processes are interesting because the yields are expected to be higher. The suitable energy ranges for the production of ^{22}Na by these three processes, the expected thick target yields and typical batch yields achieved (if available) are given in Table 2.

For practical production of ^{22}Na, the $^{nat}Mg(d,x)^{22}Na$ process (involving mainly the low-energy $^{24}Mg(d,\alpha)^{22}Na$ reaction) with about 15 MeV deuterons has been in use for more than 50 years. The chemical separation of ^{22}Na in no-carrier-added form is generally performed by cation-exchange chromatography [cf. 40, 41]. In a typical experiment, a 4 h irradiation at a beam current of 25 μA led to a ^{22}Na batch yield of about 7 MBq [40]. Longer irradiation times, higher beam currents and use of an isotopically enriched ^{24}Mg target considerably enhance the product yield. Very recently, a high-current gas target has been developed to produce ^{22}Na via another low-energy reaction, namely $^{nat}Ne(p,x)^{22}Na$ [42]. The calculated thick target yield of this reaction over $E_p = 15 \rightarrow 6$ MeV amounts to 0.028 MBq/μAh. After filling the target with Ne gas up to 12 bar, irradiation was carried out with 17 MeV protons at 5 μA for 6 days. Thereafter the evacuated target was rinsed with a dilute solution of NaOH. The batch yield of ^{22}Na amounted to 11 MBq [42]. By using highly enriched ^{22}Ne gas as target material (instead of ^{nat}Ne), the batch yield of ^{22}Na could be significantly increased. The third low-energy reaction is ^{19}F(α,n)^{22}Na. The calculated thick target yield of this reaction over $E_\alpha = 14 \rightarrow 4$ MeV amounts to 0.022 MBq/μAh. It has also been used to produce tracer amounts of ^{22}Na at α-particle energies of < 15 MeV.

Relatively large amounts of ^{22}Na have been produced to date using the ^{27}Al(p,3p3n)^{22}Na and ^{nat}Mg(p,x)^{22}Na processes induced by intermediate energy protons. In a typical experiment, a thick Al target irradiated with 146 MeV protons was transferred to a crucible placed in a distillation apparatus, and heated to 1200 – 1300 K. The radiosodium was removed from the molten target by a He stream and collected in 0.1 M HCl. The batch yield of ^{22}Na amounted to 1.3 GBq [43]. Similar amounts of ^{22}Na activity have been produced at the Los Alamos National Laboratory (LANL, USA). In a specialized variation of the technique, used in preparation of a source for astrophysical studies, the radiosodium atoms released from the molten target were ionized, extracted as an ion beam and directed to a collector foil by a mass spectrometric system. As expected, the batch yield in this case was much lower, amounting only to 0.22 MBq [44]. As far as the use of the ^{nat}Mg(p,x)^{22}Na reaction to produce ^{22}Na is concerned, a thick target yield measurement of ^{22}Na after a 2 h irradiation of Mg with 70 MeV protons delivered a value of 2.54 MBq [45]. The highest amount of ^{22}Na activity is, however, produced at the iThemba Labs (S.A.). After irradiation of a Mg target for several weeks with protons over the energy range $E_p = 61 \rightarrow 40$ MeV at a beam current of 80 μA, the radiosodium was separated by cation-exchange chromatography. The batch yield of ^{22}Na amounted to 11 GBq [46].

Summarizing the production possibilities of ^{22}Na, it may be stated that tracer amounts of this radionuclide can be conveniently obtained via the three relatively low-energy processes, namely ^{19}F(α,n)^{22}Na, ^{nat}Ne(p,x)^{22}Na and ^{nat}Mg(d,x)^{22}Na. A medium-sized cyclotron like the CPX 30 (IBA, Louvain-La-Neuve, Belgium), is well suited for this purpose. Large amounts of ^{22}Na, however, can be produced only via the ^{27}Al(p,3p3n)^{22}Na and ^{nat}Mg(p,x)^{22}Na processes at an intermediate energy accelerator wit $E_p \geq 70$ MeV. Furthermore, regarding the quality of ^{22}Na, it is emphasized that the demands are high even though the major applications are in materials research. Of particular interest are the radionuclidic purity, the chemical purity and the specific activity. The presence of all other elements as chemical impurities in the vicinity of the radionuclide ^{22}Na influences the electron density and could be very disturbing in studies on materials properties.

The radionuclides **^{68}Ga** and **^{82}Rb** are also standard positron emitters, being widely used in patient care. The radionuclide ^{68}Ga finds application also in materials research. Those two radionuclides are obtained via generator systems. Their long-lived parents ^{68}Ge ($T_{½}$ = 271 d) and ^{82}Sr ($T_{½}$ = 25.3 d), respectively, are produced using intermediate energy protons.

For the production of ^{68}Ge, generally a ^{nat}Ga target is used. The suitable proton energy range is E_p = 70 → 20 MeV [2]. In a typical experiment gallium metal encapsulated in niobium was irradiated with 100 MeV protons and the radiogermanium, formed via the ^{nat}Ga(p,xn)-process, was extracted as $GeCl_4$ in toluene, benzene, etc. after dissolving the target. Further purification of ^{68}Ge was performed by several extraction and back-extraction cycles. The batch yield of ^{68}Ge corresponded to about 20 GBq and its radionuclidic purity was > 99% [47]. Further improvements have led to batch yields of up to 40 GBq of ^{68}Ge.

For the preparation of the ^{68}Ge/^{68}Ga generator, the separated ^{68}Ge is generally loaded on a tin oxide column, and the positron emitting daughter ^{68}Ga, formed by the decay of ^{68}Ge, is periodically eluted with 1 M HCl. Optimisation studies have led to a very efficient processing of the ^{68}Ga-eluate for medical application [48].

With regard to the production of ^{82}Sr, previously the ^{85}Rb(p,4n)-reaction using an enriched ^{85}Rb target was employed but recently, for economic reasons, more use has been made of ^{nat}Rb as target material. This, however, leads to the formation of appreciable amounts of the longer lived impurity ^{85}Sr ($T_{½}$ = 64.9 d) as well. The excitation functions for the formation of both ^{82}Sr and ^{85}Sr in proton induced reactions on ^{nat}Rb are shown in Fig. 4. From those data it is concluded that the optimum energy range for the production of ^{82}Sr is E_p = 70 → 50 MeV [49]. Over this energy range the ratio of ^{85}Sr to ^{82}Sr amounts to 0.25 which is tolerable. The target for irradiation generally consists of RbCl encapsulated in stainless steel. The wet chemical processing of the irradiated target is based on ion-exchange chromatography. The batch yield of ^{82}Sr corresponds to about 70 GBq [cf. 50].

For the preparation of the ^{82}Sr/^{82}Rb generator system, the separated ^{82}Sr is loaded on a suitable column (e.g. Chelex 100 chelating resin, Dowex-1 anion exchange resin) and purged with an eluent. The daughter ^{82}Rb is then periodically eluted with saline. Regarding the quality of the separated ^{82}Sr, a vigilant watch on the integrity of the column against ^{85}Sr breakthrough is necessary.

4.2 Non-standard positron emitters

4.2.1 General

Non-standard positron emitters are needed for studying slow biological functions. A few radionuclides are also used in ***radioimmunotherapy***. Many β^+ emitting radionuclides attached to an antibody are promising diagnostic and therapeutic agents. Several other non-standard positron emitters are now finding application in ***theranostics***. This entails a combination of diagnosis and internal radionuclide therapy. By combining a β^+ and a β^- (or Auger electron or α-particle) emitting pair of radionuclides of a given element in the same chemical form, it is possible to measure the uptake kinetics by PET imaging, thereby allowing an accurate dosimetric calculation related to therapy. It was first applied in the case of internal therapy with ^{90}Y after mixing it with the positron emitter ^{86}Y [51]. Today, several pairs are finding great interest [52]. A yet another application of non-standard positron emitters is in ***multimodal imaging***. This stipulates a combination of two or more imaging techniques. For example PET can be combined with magnetic resonance imaging (MRI) using one agent bearing two signal transmitters. This combination is particularly interesting due to quantitative nature of PET and high resolution of MRI.

The non-standard positron emitters were periodically reviewed [53-56]. Later on various aspects of development work were elucidated [57] and an updated review discussed some further work [58]. More recently, a comprehensive review covered all medically useful or potentially useful positron emitters [2], describing the common production routes, the optimum energy ranges deduced, and the thick target yields, calculated from the excitation functions, together with a list of all relevant references to nuclear data. In the present review therefore only a short summary of the important non-standard positron emitters and their applications is presented (cf. Table 3). Some salient features relevant to their clinical scale production are enumerated below.

In general, most of the non-standard positron emitters are produced via a low-energy (p,n), (p,α) or (d,n) reaction on an isotopically highly enriched solid target. A few examples of the radionuclides produced are ^{55}Co, ^{61}Cu, ^{64}Cu, ^{86}Y, ^{120}I, ^{124}I, etc. [cf. 59-64]. The exceptions are ^{45}Ti and ^{89}Zr where the natural target material is monoisotopic. The expensive enriched material has to be economically handled. Furthermore, there is the constraint of low particle energy. This calls upon ingenuity in target preparation and recovery of the enriched material for reuse.

Many of the nuclear reaction cross section data were measured at the Forschungszentrum Jülich but the other development work was carried out at several other laboratories as well. In those studies, electrochemical deposition [cf. 59, 61, 63], melting [cf. 64-67], pressed pellet formation [cf. 60, 62, 68,69,71] and alloy formation [cf. 70] have been often used for preparation of high-current irradiation targets. Efficient chemical separation methods were applied to isolate the desired positron emitter in high purity and high specific activity. For this purpose, a large number of methods have been developed, for example, dry distillation for ^{120}I and ^{124}I [cf. 64-67, 69], thermochromatography for ^{76}Br and ^{94m}Tc [cf. 70, 71], ion-exchange chromatography for ^{64}Cu and ^{124}I [cf. 61, 72-74], solvent extraction for ^{66}Ga, ^{86}Y and ^{124}I [cf. 75-77], etc. The successful use of a low-energy (p,n) reaction to produce a non-standard positron emitter at a medical cyclotron has also led to the development of the so-called ***solution target*** in which a solution of the enriched target isotope is irradiated, instead of a solid target. This technology has been successfully developed for the production of a few non-standard positron emitters, e.g. ^{44}Sc [78], ^{86}Y [79], ^{89}Zr [80], etc. It is, however, necessary to take care of the irradiation-induced chemical species [cf. 80]. The yield of the desired radionuclide is generally low but it may be enough for local use. As a special case some low melting target materials have been irradiated in molten form using a vertical beam [cf. 81].

Despite the successful application of the low-energy (p,n) reaction to produce a large number of non-standard positron emitters at a medical cyclotron, the development of a few other novel positron emitters demands the use of intermediate energy nuclear reactions. A few examples are ^{52}Fe, ^{73}Se, ^{83}Sr, ^{152}Tb, etc. They can be produced via (p,xn) reactions at a high-intensity cyclotron, accelerating protons to energies up to 100 MeV [cf. 2]. Some work on those radionuclides is progressing in a few laboratories. At those charged-particle beam energies, there is some flexibility in target construction because thicker foils and stronger cooling circuits can be utilized. Furthermore, highly enriched targets are not as often used as in the case of low-energy production processes. It should also be mentioned that a few non-standard positron emitters are advantageously produced using the α-particle beam, e.g. ^{30}P, ^{38}K, ^{34m}Cl, etc. (for a review cf. [82]).

A few novel and potentially useful positron emitters could possibly be obtained from generators. Some of them are ^{44}Ti (59.1a)/^{44}Sc (3.9 h), ^{72}Se (8.5 d)/^{72}As (26.0 h) and ^{140}Nd (3.4d)/^{140}Pr (3.4 min). The production of all those parent nuclides can only be conducted by using intermediate energy reactions.

4.2.2 Established non-standard positron emitters

Out of all non-standard positron emitters listed in Table 3, four of them, namely ^{64}Cu, ^{86}Y, ^{89}Zr and ^{124}I, are finding broader interest and they may be regarded as established non-standard positron emitters. They are all suitable for PET imaging, although in the case of ^{86}Y strong γ-ray scattering corrections need to be applied. There are numerous applications of those radionuclides in organ function studies. The radionuclides ^{64}Cu, ^{89}Zr and ^{124}I are partly used in radioimmunotherapy as well. The major use of ^{64}Cu, ^{86}Y and ^{124}I, however, is in theranostics, i.e. in combination with their respective β^- emitting therapeutic partners, namely ^{67}Cu ($T_{½}$ = 2.58 d), ^{90}Y ($T_{½}$ = 2.7 d) and ^{131}I ($T_{½}$ = 8.02 d), respectively. The most established pair is ^{86}Y/^{90}Y, although ^{86}Y is not ideal for PET imaging (as mentioned above). The pair ^{124}I/^{131}I has found broad application but ^{124}I is somewhat long-lived and rather expensive. Nevertheless, occasionally ^{124}I is used alone both as a PET radionuclide and a therapeutic nuclide. The pair ^{64}Cu/^{67}Cu would be ideal but so far ^{67}Cu is not readily available. Thus, all three theranostic pairs demand further development work. However, as far as the availability of the above mentioned four positron emitters is concerned, clinical scale quantities are produced via the (p,n) reaction in a large number of laboratories (for original references see earlier reviews [57, 58]). Large scale productions of those four established non-standard positron emitters are now being realized by several commercial companies.

4.2.3 Emerging non-standard positron emitters

Many of the non-standard positron emitters listed in Table 3 are of great importance but their use is so far not as pronounced as of the established positron emitters described above. Some of them have gained more importance in recent years and could be termed as emerging positron emitters. They include ^{44g}Sc, ^{45}Ti, ^{52g}Mn, ^{73}Se and ^{152}Tb. The major interest in ^{44g}Sc and ^{152}Tb is in their possible use in theranostics, i.e. in combination with their respective β^- emitting therapeutic partners, namely ^{47}Sc ($T_{½}$ = 3.35 d) and ^{161}Tb ($T_{½}$ = 6.9 d). The pair ^{44g}Sc/^{47}Sc would be ideal. Although a clinical scale production of ^{44g}Sc via the ^{44}Ca(p,n)-reaction has been developed, so far ^{47}Sc is not readily available. The pair ^{152}Tb/^{161}Tb, on the other hand, is somewhat exotic. Whereas ^{161}Tb can be produced in a nuclear reactor, the positron emitter ^{152}Tb has hitherto been obtained only via on-line mass separation from the spallation products of Ta with high energy protons. The production of both those pairs has been recently reviewed in detail [52]. It is therefore not treated in this review. The interest in ^{73}Se relates to metabolic investigations of inorganic and seleno-organic compounds using PET. Furthermore, since selenium is an analogue of sulphur, which itself has no suitable positron emitting radionuclide, the radionuclide ^{73}Se could be utilized in the study of sulphur metabolism as well. The production of ^{73}Se is generally carried out via the ^{75}As(p,3n)-reaction at an intermediate energy cyclotron and is therefore not readily available. The various methods of its production have also been very recently reviewed [58]. In the present article, therefore, we will discuss only the production methodologies of ^{45}Ti and ^{52g}Mn. For those two radionuclides some new development work carried out in recent years in our laboratory is reported.

^{45}Ti ($T_{½}$ = 3.1 h)

This radionuclide has decay properties very suitable for PET studies (half-life, high positron emission intensity, medium positron energy, almost no γ-ray). Due to its tetravalent character, titanium forms interesting Ti(IV) complexes, particularly titanocene complexes, which exhibit high antitumour activity. This radionuclide is thus of potential interest in tumour research.

For the production of ^{45}Ti, generally the ^{45}Sc(p,n)^{45}Ti reaction has been used. The measured cross section data [83, 84] show scatter but an eye-guided curve could be drawn through the more consistent data. The excitation functions of the ^{45}Sc(d,2n)^{45}Ti and ^{52}Ca(α,n)^{45}Ti reactions have also been reported [85, 86]. We calculated the expected thick target yields of ^{45}Ti from the excitation curves for the (p,n) and (α,n) reactions for 1 h irradiation, but adopted the calculated values for the (d,2n) reaction from Ref. [85]. The results are reproduced in Fig. 5. Evidently the low-energy (p,n) reaction is most suitable for the production of ^{45}Ti. The optimum energy range deduced is E_p = 14.5 → 5 MeV and the calculated yield amounts to 433 MBq/µAh.

In typical production experiments [87-89], Sc foil was irradiated with 14.5 MeV protons at about 10 µA beam current. Thereafter the foil was dissolved in 6 M HCl and ^{45}Ti was separated by cation-exchange chromatography. Typically the batch yield of ^{45}Ti amounted to about 2 GBq and its radionuclidic purity to 99.8%. Recently a continuous liquid-liquid extraction using membrane based separator was utilized for the separation of [^{45}Ti]$TiCl_4$. [90] A further new strategy for the separation of ^{45}Ti has been developed in our laboratory. It involves the thermochromatographical removal of radiotitanium from the irradiated Sc in the form of [^{45}Ti]$TiCl_4$ [91]. Further optimization work with regard to the quality of the separated product and its use in preparing suitable ^{45}Ti-complexes is in progress.

^{52g}Mn ($T_{½}$ = 5.6 d)

This radionuclide is of great importance in multimodal imaging, especially in combining PET with MRI, because Mn is used as a contrast agent in MRI. Authentic tracers labelled with ^{52g}Mn have been prepared [92, 93] and thus the significance of this radionuclide is increasing. The radionuclide ^{52g}Mn ($I = 6^+$) has also a higher lying isomeric state ^{52m}Mn ($T_{½}$ = 21.0 min; $I = 2^+$). It decays > 97 % by β^+emission to stable ^{52}Cr and < 2% to the ground state ^{52g}Mn. The isomeric cross section ratio for the formation of the two states was determined in five different reactions and a systematic analysis was performed [94]. At low energies (< 10 MeV) the short-lived ^{52m}Mn is favoured because of its low spin but at higher energies (> 15 MeV) the yield of the longer lived ^{52g}Mn increases considerably due to its higher spin. In order to avoid ambiguities in PET scans, it is recommended to use the longer lived ^{52g}Mn after the complete decay of ^{52m}Mn.

For the production of ^{52g}Mn several nuclear reactions were investigated (for an early review see [25]), out of which the ^{52}Cr(p,n)-reaction was found to be the most suitable. Since the ^{52}Cr(p,2n)^{51}Mn ($T_{½}$ = 46.2 min) and ^{50}Cr(p,n)^{50}Mn ($T_{½}$ = 1.8 min) reaction products are short-lived, it is not absolutely necessary to use an enriched ^{52}Cr target. Most of the studies have, therefore, been carried out using ^{nat}Cr as target material. The results of the nuclear reaction cross section measurements [95-100] are shown in Fig. 6. The optimum energy range for the production of ^{52g}Mn is deduced to be $E_p = 17 \rightarrow 8$ MeV; its calculated yield amounts to 14 MBq/µAh. The estimated impurity level of ^{54}Mn ($T_{½}$ = 312.2 d) formed via the ^{54}Cr(p,n)^{54}Mn reaction on the 2.36 % ^{54}Cr present in ^{nat}Cr amounts to about 0.25%. If this level is not tolerable, it would be mandatory to use an enriched ^{52}Cr target.

The target for irradiation consists of either enriched ^{52}Cr or ^{nat}Cr, electroplated on a Au backing, or simply a high-purity chromium disk. Irradiation is generally carried out for a few hours using a proton beam of up to 20 µA on a slanting [cf. 65]. For the separation of n.c.a. ^{52g}Mn from the bulk of chromium, several methods have been reported, based mainly on co-precipitation and anion-exchange chromatography. Some improvements have been introduced in recent years [65, 101-104]. In a novel method [99] the chemical processing starts by dissolution of the target in HCl at 70 °C followed by reduction of radiomanganese to Mn^{2+}, and finally applying chromatography. The typical batch yield of the obtained [^{52g}Mn]$MnCl_2$ was ca. 150 MBq. Intensified efforts are presently being devoted in several laboratories to produce this radionuclide in larger quantities.

5. Concluding remarks

Radioactive elements constitute a significant part of the present Periodic Table of Elements. Furthermore, radioisotopes are important players in its background being highly relevant to life science and materials research. The property of α–particle emission from many heavy mass nuclei makes them attractive for α-targeted therapy. In the region of the lightest mass elements, on the other hand, the neutron deficient radionuclides decay predominantly by positron emission. With the increasing charge of the nucleus, the competition between positron emission and electron capture increases, the latter becoming the most dominant decay mode in the region of rare earths and heavier mass elements. The annihilation of a positron is utilized in materials research, in quantitative imaging of organs as well as in determination of metabolic turnover rates in plants and humans.

Each application needs a suitable positron emitter. In materials research the origin of the positron is not important. It may come from a commonly used ^{22}Na source or from an accelerator delivering hard photons which generate positrons via pair production. In plant physiological studies, mainly ^{11}C finds wide application. For medical use, however, a large number of positron emitters attached to very specific chemical molecules are needed. Some standard radionuclides are routinely produced in hospital environments for patient care, but work is underway to develop novel β^{+} emitters for new emerging medical applications. Although most of the β^{+} emitters are produced using low- and medium-sized cyclotrons, the necessity of availability of intermediate energy proton accelerators is increasing to be able to produce unusual β^{+} emitting isotopes of the heavier mass elements.

The periodicity of the Periodic Table of Elements is reflected to some extent in the uptake of radionuclides and radiopharmaceuticals by living systems. Alkali and alkali-like metals (e.g. the positron emitters ^{38}K and ^{82g}Rb, and the γ-ray emitter $^{201}Tl^{+1}$) find application in cardiac blood flow studies. Other examples are the specific attachment of β^{+} emitters of trivalent metals (e.g. ^{44g}Sc, ^{86}Y, lanthanides) to tumour seeking agents or of halogens to biomolecules (via an analogue approach) for study of metabolic processes.

In summary, it may be stated that the radionuclide development work constitutes a very versatile and dynamic area of research related to non-energy applications of nuclear sciences. In view of enhancing interest in human health, the future perspectives of this field thus appear to be very promising.

References

1. Stöcklin, G., Qaim, S.M., Rösch, F.: The impact of radioactivity on medicine. Radiochim. Acta **70/71**, 249–272 (1995).
2. Qaim, S.M.: Nuclear data for production and medical application of radionuclides: Present status and future needs. Nucl. Med. Biol. **44**, 31-49 (2017).
3. Evaluated Nuclear Structure and Decay Data File (ENSDF), BNL, USA. Available online: www.nnds.bnl.gov/ensdf (accessed on 6 June 2017).
4. Kuhn, S., Spahn, I., Scholten, B., Coenen, H.H.: Positron and gamma-ray intensities in the decay of ^{45}Ti. Radiochim. Acta **103**, 403-409 (2015).
5. Qaim, S.M., Bisinger, T., Hilgers, K., Nayak, D., Coenen, H.H.: Positron emission intensities in the decay of ^{64}Cu, ^{76}Br and ^{124}I. Radiochim. Acta **95**, 67-73 (2007).
6. Hohn, A., Coenen, H.H., Qaim, S.M.: Positron emission intensity in the decay of ^{120g}I. Radiochim. Acta **88**, 139-141 (2000).
7. Anderson, C.D.: The positive electron. Phys. Rev. **43**, 491-494 (1933).
8. Berko, S., Zuckerman, J.: Polarized positron annihilation in ferromagnets. Phys. Rev. Lett. **13**, A339 (1964).
9. Callewaert, V., Shastry, K., Saniz, R., Makkonen, I., Barbiellini, B., Assaf, B.A., Heiman, D., Moodera, J.S., Partoens, B., Bansil, A., Weiss, A.H.: Positron surface state as a spectroscopic probe for characterizing surfaces of topological insulator materials. Phys. Rev. B **94**, 115411 (2016).
10. Singh, A.N.: Positron annihilation spectroscopy in tomorrow's material defect studies. Appl. Spectroscopy Rev. **51**, 359-378 (2016).
11. Cizek, J.: Characterization of lattice defects in metallic materials by positron annihilation spectroscopy: A review. J. Mater. Sci. Tech. **34**, 577-598 (2018).
12. Ravn, H., Schulte, W.H., Rolfs, C., Waanders, F.B., Kavanagh, R.W.: Production of ^{22}Na Targets or Positron Sources by Means of Ion-Implantation. Nucl. Instrum. Meth. B **58**, 174-178 (1991).
13. Saito, F., Hyodo, T., Nagashima, Y., Kurihara, T., Suzuki, N., Itoh, Y., Goto, A.: Intense radioisotope sources for spin polarized positron beams. “New Directions in Antimatter Chemistry and Physics”, edited by C.M. Surko and F.A. Gianturco (Kluwer, The Netherlands, 2001) pp. 35-45.

14. Wada, K., Miyashita, A., Maekawa, M., Sakai, S., Kawasuso, A.: Spin-polarized positron beams with ^{22}Na and ^{68}Ge and their applications to materials research. Proc. of International Workshop on Physics with Positrons at Jefferson Lab, 04001 **1970**, (2018).
15. Jahnke, S., Menzel, M.I., van Dusschoten, D., Roeb, G.W., Bühler, J., Minwuyelet, S., Blümler, P., Temperton, V.M., Hombach, T., Streun, M., Beer, S., Khodaverdi, M., Ziemons, K., Coenen, H.H., Schurr, U.: Combined MRI-PET dissects dynamic changes in plant structures and functions. The Plant Journal **59**, 634-644 (2009).
16. De Schepper, V., Bühler, J., Thorpe, M., Roeb, G., Huber, G., van Dusschoten, D., Jahnke, S., Steppe, K.: ^{11}C-PET imaging reveals transport dynamics and sectorial plasticity of oak phloem after girdling. Plant Science **4**, article 200 (2013).
17. Hanik, N., Gómez, S., Schueller, M., Orians, C.M., Ferrieri, R.A.: Use of gaseous $^{13}NH_3$ administered to intact leaves of *nicotiana tabacum* to study changes in nitrogen utilization during defence induction. Plant, Cell and Environment **33**, 2173-2179 (2010).
18. Agtuca, B., Rieger, E., Hilger, K., Song, L.H., Robert, C.A.M., Erb, M., Karve, A., Ferrieri, R.A.: Carbon-11 reveals opposing roles of auxin and salicylic acid in regulating leaf physiology, leaf metabolism, and resource allocation patterns that impact root growth in *zea mays*. J. Plant Growth Regul. **33**, 328-339 (2014).
19. Ishioka, N.S., Matsuoka, H., Watanabe, S., Osa, A., Koizumi, M., Kume, T., Matsuhashi, S., Fujimura, T., Tsuji, A., Uchida, H., Sekine, T.: Production of positron emitters and application of their labeled compounds to plant studies. J. Radioanal. Nucl. Chem. **239**, 417-421 (1999).
20. Kawachi, N., Sakamoto, K., Ishii, S., Fujimaki, S., Suzui, N., Ishioka, N.S., Matsuhashi, S.: Kinetic analysis of carbon-11-labeled carbon dioxide for studying photosynthesis in a leaf using positron emitting tracer imaging system. IEEE Trans. Nucl. Sci. **53**, 2991-2997 (2006).
21. Nakanishi, T.M.: What you can see by developing real-time radioisotope imaging system for plants: from water to element and CO_2 gas imaging. J. Radioanal. Nucl. Chem. **318**, 1689-1695 (2018).
22. Harpen, M.D.: Positronium: Review of symmetry, conserved quantities and decay for the radiological physicist. Med Phys **31**, 57-61 (2004).

23. Herzog, H., Tellmann, L., Scholten, B., Coenen, H.H., Qaim, S.M.: PET imaging problems with the non-standard positron emitters ^{86}Y and ^{124}I. Quart. J. Nucl. Med. Mol. Imaging **52**, 159–165 (2008).

24. Qaim, S.M.: Medical Radionuclide Production. De Gruyter, Berlin, 2019.

25. Qaim, S.M.: Nuclear data relevant to cyclotron produced short-lived medical radioisotopes. Radiochim. Acta **30**, 147-162 (1982).

26. Qaim, S.M., Clark, J.C., Crouzel, C., Guillaume, M., Helmeke, H.J., Nebeling, B., Pike, V.W., Stöcklin, G.: PET radionuclide production, in Radiopharmaceuticals for Positron Emission Tomography–Methodological Aspects (G. Stöcklin, V.W. Pike, Editors), Kluwer, Dordrecht, 1993, pp.1–43.

27. Charged Particle Cross Section Database for Medical Radioisotope Production: Diagnostic Radioisotopes and Monitor Reactions. IAEA-TECDOC-1211, IAEA, Vienna, Austria, 2001, for later updates see www-nds.iaea.org/medical/.

28. Hess, E., Takács, S., Scholten, B., Tárkányi, F., Coenen, H.H., Qaim, S.M.: Excitation function of the $^{18}O(p,n)^{18}F$ nuclear reaction from threshold up to 30 MeV. Radiochim. Acta **89**, 357–362 (2001).

29. Qaim, S.M.: The present and future of medical radionuclide production. Radiochim Acta **100**, 635-651 (2012).

30. Kovács, Z., Scholten, B., Tárkányi, F., Coenen, H.H., Qaim, S.M.: Cross section measurements using gas and solid targets for production of the positron-emitting radionuclide O-14. Radiochim. Acta **91**, 185–189 (2003).

31. Szücs, Z., Hamkens, W., Takács, S., Tárkányi, F., Coenen, H.H., Qaim, S.M.: Excitation functions of $^{14}N(d,t)^{13}N$ and $^{14}N(d,\alpha n)^{11}C$ reactions from threshold to 12.3 MeV: radionuclidic purity of ^{15}O produced via the $^{14}N(d,n)^{15}O$ reaction. Radiochim. Acta **80**, 59–63 (1998).

32. Suzuki, K., Yamazaki, T., Sasaki, M., Kubodera, A.: Specific activity of $[^{11}C]CO_2$ generated in a N_2 gas target: effect of irradiation dose, irradiation history, oxygen content and beam energy. Radiochim. Acta **88**, 211–215 (2000).

33. Blessing, G., Coenen, H.H., Franken, K., Qaim, S.M.: Production of $[^{18}F]F_2$, $HF(^{18}F)$ and $^{18}F(aq)$ using the $^{20}Ne(d,\alpha)^{18}F$ process. Int. J. Appl. Radiat. Isot. **37**, 1135–1139 (1986).

34. Roberts, A.D., Oakes, T.R., Nickles, R.J.: Development of an improved target for $[^{18}F]F_2$ production. Appl. Radiat. Isot. **46**, 87–91 (1995).

35. Bishop, A., Satyamurthy, N., Bida, G., Phelps, M., Barrio, J.R.: Identification and quantitation of gaseous compounds of fluorine generated in [^{18}F]F_2 target systems. Nucl. Med. Biol. **23**, 391–405 (1996).

36. Hess, E., Blessing, G., Coenen, H.H., Qaim, S.M.: Improved target system for production of high purity [^{18}F]fluorine via the ^{18}O(p,n)^{18}F reaction. Appl. Radiat. Isot. **52**, 1431–1440 (2000).

37. Forsback, S., Solin, O.: Post-target produced [^{18}F]F_2 in the production of PET radiopharmaceuticals. Radiochim. Acta **103**, 219-226 (2015).

38. Takács, S., Tárkányi, F., Qaim, S.M.: Excitation function of ^{22}Ne(p,n)^{22}Na reaction: possibility of production of ^{22}Na at a small cyclotron. Appl. Radiat. Isot. **47**, 303-307 (1996).

39. EXFOR (Experimental Nuclear Reaction Data File) Database Version of 2019, IAEA, Vienna, https://www-nds.iaea.org/exfor/exfor.htm

40. de Britto, J.L.Q., Bastos, M.A.V., da Silva, R.F., da Silva, A.G.: Production of no-carrier-added residue free ^{22}Na. J. Radioanal. Nucl. Chem. Letters **127**, 31-36 (1988).

41. Brits, R.J.N., Toerien, F.V.: The separation of ^{22}Na from Mg by cation-Exchange on a macroporous resin. Appl. Radiat. Isot. **39**, 1045-1050 (1988).

42. Mandal, B.C., Barua, L., Das, S.S., Pal, G.: Development of a Ne gas target for ^{22}Na production by proton irradiation. Rev. Sci. Instr. **87**, 033304 (2016).

43. Kir'yanov, B.S., Lastov, A.I., Moseev, L.I., Mamonov, A.N., Razbash, A.A., Sevast'yanov, Y.G.: Distillation ^{22}Na separation from proton-irradiated aluminum targets. Atomic Energy **88**, 233-235 (2000).

44. Dauria, J.M., Dombsky, M., Buchmann, L., Vincent, J.S.: Studies Related to the Production of an isotopically pure ^{22}Na radioactive target. Nucl. Instrum. Meth. A **288**, 354-359 (1990).

45. Haasbroek, F.J., Steyn, J., Neirinckx, R.D., Burdzik, G.F., Cogneau, M., Wanet, P.: Thick target yields of Na-22 in magnesium, Fe-55 in cobalt, Co-56, Co-57 and Co-58 in nickel and Hf-176 in tantalum by proton bombardment in energy range up to 100 MeV. Int. J. Appl. Radiat. Isot. **28**, 533-534 (1977).

46. Naidoo, C., van der Meulen, N.P., Vermeulen, C., Krause-Rehberg, R.: The production of ^{22}Na positron sources at iThemba Labs. Poster at 16th Int. Conference on Positron Annihilation (ICPA-16), Bristol, United Kingdom, 2012, Editor: A. Alan, Journal of Physics, Conference Series Volume 443, 2013.

47. Meinken, G.E., Kurczak, S., Mausner, L.F., Kolsky, K.L., Srivastava, S.C.: Production of high specific activity ^{68}Ge at Brookhaven National Laboratory. J. Radioanal. Nucl. Chem. **263**, 553–557 (2005).
48. Rösch, F., Riss, P.J.: The renaissance of the 68Ge/68Ga radionuclide generator initiates new developments in 68Ga radiopharmaceutical chemistry. Curr. Top. Med. Chem. **10**, 1633–1668 (2010).
49. Qaim, S.M., Steyn, G.F., Spahn, I., Spellerberg, S., van der Walt, T.N., Coenen, H.H.: Yield and purity of ^{82}Sr produced via the ^{nat}Rb(p,xn)^{82}Sr process. Appl. Radiat. Isot. **65**, 247–252 (2007).
50. van der Meulen, N.P., van der Walt, T.N., Steyn, G.F., Raubenheimer, H.G.: The production of ^{82}Sr using larger format RbCl targets. Appl. Radiat. Isot. **72**, 96–99 (2013). Erratum: Radiat. Isot. **83,** 36 (2014).
51. Herzog, H., Rösch, F., Stöcklin, G., Lueders, C., Qaim, S.M., Feinendegen, L.E.: Measurement of pharmacokinetics of ytrrium-86 radiopharmaceuticals with PET and radiation dose calculation of analogous yttrium-90 radiotherapeutics. J. Nucl. Med. **34**, 2222–2226 (1993).
52. Qaim, S.M., Scholten, B., Neumaier, B.: New developments in the production of theranostic pairs of radionuclides. J. Radioanal. Nucl. Chem. **318**, 1493–1509 (2018).
53. Pagani, M., Stone-Elander, S., Larsson, S.A.: Alternative positron emission tomography with non-conventional positron emitters: effects of their physical properties on image quality and potential clinical applications. Eur. J. Nucl. Med. **24**, 1301-1327 (1997).
54. Nickles, R.J.: The production of a broader palette of PET tracers. J. Lab. Compd. Radiopharm. **46**, 1-27 (2003).
55. McQuade, P., Rowland, D.J., Lewis, J.S., Welch, M.J.: Positron-emitting isotopes produced on biomedical cyclotrons. Curr. Med. Chem. **12**, 807-818 (2005).
56. Qaim, S.M.: Decay data and production yields of some non-standard positron emitters used in PET. J. Nucl. Med. Mol. Imaging **52**, 111-120 (2008).
57. Qaim, S.M.: Development of novel positron emitters for medical applications: nuclear and radiochemical aspects. Radiochim. Acta **99**, 611-625 (2011).
58. Qaim, S.M., Spahn, I.: Development of novel radionuclides for medical application. J. Label. Compd. Radiopharm. **61**, 126–140 (2018).

59. Spellerberg, S., Reimer, P., Blessing, G., Coenen, H.H., Qaim, S.M.: Production of ^{55}Co and ^{57}Co via proton induced reactions on highly enriched ^{58}Ni. Appl. Radiat. Isot. **49**, 1519–1522 (1998).

60. Zaman, M.R., Spellerberg, S., Qaim, S.M.: Production of ^{55}Co via the $^{54}Fe(d,n)$-process and excitation functions of $^{54}Fe(d,t)^{53}Fe$ and $^{54}Fe(d,\alpha)^{52m}Mn$ reactions from threshold up to 13.8 MeV. Radiochim. Acta **91**, 105–108 (2003).

61. Szelecsényi, F., Blessing, G., Qaim, S.M.: Excitation functions of proton induced nuclear reactions on enriched ^{61}Ni and ^{64}Ni: possibility of production of no-carrier-added ^{61}Cu and ^{64}Cu at a small cyclotron. Appl. Radiat. Isot. **44**, 575–580 (1993).

62. Rösch, F., Qaim S.M., Stöcklin, G.: Nuclear data relevant to the production of the positron emitting radioisotope ^{86}Y via the $^{86}Sr(p,n)$- and $^{nat}Rb(^{3}He,xn)$-processes. Radiochim. Acta **61**, 1–8 (1993).

63. Scholten, B., Kovács, Z., Tárkányi, F., Qaim, S.M.: Excitation functions of $^{124}Te(p,xn)^{123,124}I$ reactions from 6 MeV to 31 MeV with special reference to the production of ^{124}I at a small cyclotron. Appl. Radiat. Isot. **46**, 255–259 (1995).

64. Qaim, S.M., Hohn, A., Bastian, T., El-Azoney, K.M., Blessing, G., Spellerberg, S., Scholten, B., Coenen, H.H.: Some optimisation studies relevant to the production of high-purity ^{124}I and ^{120g}I at a small-sized cyclotron. Appl. Radiat. Isot. **58**, 69–78 (2003).

65. Spellerberg, S., Scholten, B., Spahn, I., Bolten, W., Holzgreve, M., Coenen, H.H., Qaim, S.M.: Target development for diversified irradiations at a medical cyclotron. Appl. Radiat. Isot. **104**, 106–112 (2015).

66. Nye, J.A., Avila-Rodriguez, M.A., Nickles, R.J.: Production of [^{124}I]-iodine on an 11 MeV cyclotron. Radiochim. Acta **94**, 213–216 (2006).

67. Sheh, Y., Koziorowski, J., Balatoni, J., Lom, C., Dahl, J.R., Finn, R.D.: Low energy cyclotron production and chemical separation of "no carrier added" iodine-124 from a reusable, enriched tellurium-124 dioxide/aluminum oxide solid solution target. Radiochim. Acta **88**, 169–173 (2000).

68. Kettern, K., Linse, K.H., Spellerberg, S., Coenen, H.H., Qaim, S.M.: Radiochemical studies relevant to the production of ^{86}Y and ^{88}Y at a small-sized cyclotron. Radiochim. Acta **90**, 845–849 (2002).

69. Glaser, M., Mackay, D.B., Ranicar, A.S.O., Waters, S.L., Brady, F., Luthra, S.K.: Improved targetry and production of iodine-124 for PET studies. Radiochim. Acta **92**, 951–956 (2004).

70. Tolmachev, V., Lövqvist, A., Einarsson, L., Schultz, J., Lundqvist, H.: Production of ^{76}Br by a low-energy cyclotron. Appl. Radiat. Isot. **49**, 1537–1540 (1998).

71. Rösch, F., Novgorodov, A.F., Qaim, S.M.: Thermochromatographic separation of ^{94m}Tc from enriched molybdenum targets and its large-scale production for nuclear medical application. Radiochim. Acta **64**, 113–120 (1994).

72. Dirks, C., Scholten, B., Happel, S., Zulauf, A., Bombard, A., Jungclas, H.: Characterisation of a Cu selective resin and its application to the production of ^{64}Cu. J. Radioanal. Nucl. Chem. **286**, 671-674 (2010).

73. Hassan, K.F., Spellerberg, S., Scholten, B., Saleh, Z.A., Qaim, S.M.: Development of an ion-exchange method for separation of radioiodine from tellurium and antimony and its application to the production of ^{124}I via the ^{121}Sb(α,n)-process. J. Radioanal. Nucl. Chem. **302**, 689–694 (2014).

74. Uddin, M.S., Qaim, S.M., Hermanne, A., Spahn, I., Spellerberg, S., Scholten, B., Hossain, S.M., Coenen, H.H.: Ion-exchange separation of radioiodine and its application to production of ^{124}I by alpha particle induced reactions on antimony. Radiochim. Acta **103**, 587–593 (2015).

75. Lewis, M.R., Reichert, D.E., Laforest, R., Margenau, W.H., Shefer, R.E., Klinkowstein, R.E., Hughey, B.J., Welch, M.J.: Production and purification of gallium-66 for preparation of tumor-targeting radiopharmaceuticals. Nucl. Med. Biol. **29**, 701–706 (2002).

76. Kandil, S.A., Scholten, B., Hassan, K.F., Hanafi, H.A., Qaim, S.M.: A comparative study on the separation of radioyttrium from Sr- and Rb-targets via ion-exchange and solvent extraction techniques, with special reference to the production of no-carrier-added ^{86}Y, ^{87}Y and ^{88}Y using a cyclotron. J. Radioanal. Nucl. Chem. **279**, 823–832 (2009).

77. Mandal, S., Mandal, A., Lahiri, S.: Separation of nca ^{123,124,125,126}I from alpha particle induced reactions on natural antimony trioxide target. J. Radioanal. Nucl. Chem. **292**, 579-584 (2012).

78. Hoehr, C., Oehlke, E., Bénard, F., Lee, C.J., Hou, X., Badesso, B., Ferguson, S., Miao, Q., Yang, H., Buckley, K., Hanemaayer, V., Zeisler, S., Ruth, T.J., Celler, A., Schaffer, P.: ^{44g}Sc production using a water target on a 13 MeV cyclotron. **41**, 401–406 (2014).

79. Oehlke, E., Hoehr, C., Hou, X.C., Hanemaayer, V., Zeisler, S., Adam, M.J., Ruth, T.J., Celler, A., Buckley, K., Benárd, F., Schaffer, P.: Production of Y-86 and

other radiometals for research purposes using a solution target system. Nucl. Med. Biol. **42**, 842–849 (2012).

80. Pandey, M.K., Engelbrecht, H. P., Byrne, J.F., Packard, A.B., DeGrado, T.R.: Production of ^{89}Zr via the ^{89}Y(p,n)^{89}Zr reaction in aqueous solution: effect of solution composition on in-target chemistry. Nucl. Med. Biol. **41**, 309–316 (2014).

81. Nagatsu, K., Fukada, M., Minegishi, K., Suzuki, H., Fukumura, T., Yamazaki, H., Suzuki, K.: Fully automated production of iodine-124 using a vertical beam. Appl. Radiat. Isot. **69**, 146–157 (2011).

82. Qaim, S.M., Spahn, I., Scholten, B., Neumaier, B.: Uses of alpha particles, especially in nuclear reaction studies and medical radionuclide production. Radiochim. Acta **104**, 601–624 (2016).

83. Dell, G.F., Ploughe, W.D., Hausman, H.J.: Total Reaction Cross Sections in Mass Range 45 to 65. Nucl Phys **64**, 513-523 (1965).

84. Levkovskii, N.: Middle mass nuclides (A = 40 – 100) activation cross sections by medium energy (E = 10 – 50 MeV) protons and alpha particles (experiment and systematics). Inter-Vesti, Moscow, 1991.

85. Hermanne, A., Adam Rebeles, R., Tárkányi, F., Takács, S., Takács, M.P., Csikai, J., Ignatyuk, A.: Cross sections of deuteron induced reactions on ^{45}Sc up to 50 MeV: Experiments and comparison with theoretical codes, Nucl. Instrum. Meth. B: **270**, 106-115 (2012)

86. Cheng, C.W., King, J.D.: Cross sections for the ^{42}Ca(p,γ)^{43}Sc, ^{42}Ca(α,n)^{45}Ti and ^{44}Ca(p,n)^{44}Sc reactions. J. Phys. G.: Nucl. Phys. **5**, 1261-1266 (1979).

87. Merrill, J.C., Lambrecht, R.M., Wolf, A.P.: Cyclotron isotopes and radiopharmaceuticals-XXIV. Titanium-45. Int. J. Appl. Radiat. Isot. **29**, 115–116 (1978).

88. Vávere, A.L., Laforest, R., Welch, M.J.: Production, processing and small animal PET imaging of titanium-45. Nucl. Med. Biol. **32**, 117–122 (2005).

89. Ishiwata, K., Ido, T., Monma, M., Murakami, M., Fukuda, H., Kameyama, M., Yamada, K., Endo, S., Yoshioka, S., Sato, T., Matsuzawa, T.: Potential radiopharmaceuticals labelled with titanium-45. J. Appl. Radiat. Isot. **42**, 707–712 (1991).

90. Pedersen, K.S., Imbrogno, J., Fonslet, J., Lusardi, M., Jensen, K.F., Zhuravlev,F.: Liquid–liquid extraction in flow of the radioisotope titanium-45 for positron emission tomography applications. React. Chem. Eng., 3, 898-904 (2018).

91. Giesen, K., Spahn, I., Neumaier, B.: Thermochromatographic isolation of ^{45}Ti from irradiated Sc. 2nd International Conference on Radioanalytical and Nuclear Chemistry, Budapest, Hungary, 5 May 2019 - 10 May 2019.
92. Coenen, H.H., Buchholz, M., Spahn, I., Vanasschen, C., Ermert, J., Neumaier, B.: Towards authentically labelled bi-modal PET (SPECT)/MR-probes. EJNMMI Phys. **1**, A79 (2014).
93. Vanasschen, C., Brandt, M., Ermert, J., Coenen, H.H.: Radiolabelling with isotopic mixtures of $^{52g/55}$Mn(II) as a straight route to stable manganese complexes for bimodal PET/MR imaging. Dalton Trans. **45**, 1315–1321 (2016).
94. Qaim, S.M., Sudár, S., Fessler, A.: Influence of reaction channel on the isomeric cross-section ratio. Radiochim. Acta **93**, 503–506 (2005).
95. Barrandon, J.N., Benaben, P., Debrun, J.L.: Irradiation of Elements from Z=44 to Z=82 with 10 MeV protons and application to activation analysis. Anal. Chim. Acta **83**, 157-168 (1976).
96. Walton, J. R., Heymann, D., Yaniv, A., Edgerley, D., Rowe, M. W.: Cross sections for He and Ne isotopes in natural Mg, Al, and Si, He isotopes in CaF_2, Ar isotopes in natural Ca, and radionuclides in natural Al, Si, Ti, Cr, and stainless steel induced by 12-to 45-MeV protons. J. Geophys. Res. **81**, 5689-5699 (1976)
97. Klein, A.T.J., Rösch, F., Qaim, S.M.: Investigation of ^{50}Cr(d,n)^{51}Mn and ^{nat}Cr(p,x)^{51}Mn processes with respect to the production of the positron emitter ^{51}Mn. Radiochim. Acta **88**, 253-264 (2000).
98. Titarenko, Yu. E., Batyaev, V. F., Titarenko, A. Yu., Butko, M. A., Pavlov, K. V., Florya, S. N., Tikhonov, R. S., Zhivun, V. M., Ignatyuk, A. V., Mashnik, S. G., Leray, S., Boudard, A., Cugnon, J., Mancusi, D., Yariv, Y., Nishihara, K., Matsuda, N., Kumawat, H., Mank, G., Gudowski, W.: Measurement and simulation of the cross sections for nuclide production in ^{56}Fe and ^{nat}Cr targets irradiated with 0.04- to 2.6-GeV protons. Phys. At. Nucl., **74**, 523-536 (2011)
99. Buchholz, M., Spahn, I., Scholten, B., Coenen, H.H.: Cross section measurements for the formation of ^{52}Mn and its isolation with a non-hazardous eluent. Radiochim. Acta **101**, 491-499 (2013).
100. Wooten, A.L., Lewis, B.C., Lapi, S.E.: Cross sections for (p,x) reactions on natural chromium for the production of ^{52,52m,54}Mn radioisotopes. Appl. Radiat. Isot. **96**, 154-161 (2015).

101. Lewis, C.M., Graves, S.A., Hernandez, R., Valdovinos, H.F., Barnhart, T.E., Cai, W.B., Meyerand, M.E., Nickles, R.J., Suzuki, M.: ^{52}Mn production for PET/MRI tracking of human stem cells expressing divalent metal transporter 1 (DMT1). Theranostics **5**, 227–239 (2015).

102. Buchholz, M., Spahn, I., Coenen, H.H.: Optimized separation procedure for production of no-carrier-added radiomanganese for positron emission tomography. Radiochim. Acta **103**, 893–899 (2015).

103. Graves, S.A., Hemandez, R., Fonslet, J., England, C.G., Valdovinos, H.F., Ellison, P.A., Barnhart, T.E., Elema, D.R., Theuer, C.P., Cai, W.B., Nickles, R.J., Severin, G.W.: Novel preparation methods of ^{52}Mn for immuno PET imaging. Bioconjug. Chem. **26**, 2118–2124 (2015).

104. Fonslet, J., Tietze, S., Jensen, A.I., Graves, S.A., Severin, G.N.: Optimized procedures for manganese-52: production, separation and radiolabeling. J. Appl. Radiat. Isot. **121**, 38–43 (2017).

Figure Captions

Fig. 1 Schematic representation of the positron annihilation process.

Fig. 2 Excitation functions of proton induced nuclear reactions on ^{14}N (after Kovács et al [30]).

Fig. 3 Excitation functions of nuclear reactions leading to the formation of ^{22}Na. (A) Low-energy reactions, (B) Intermediate energy reactions.

Fig. 4 Excitation functions of the reactions $^{nat}Rb(p,xn)^{85}Sr$ and $^{nat}Rb(p,xn)^{82}Sr$. For the latter process only the fitted curve is shown. (adapted from Qaim et al [49])

Fig. 5 Thick target yields of ^{45}Ti calculated from the excitation functions of $^{45}Sc(p,n)^{45}Ti$, $^{45}Sc(d,2n)^{45}Ti$ and $^{42}Ca(\alpha,n)^{45}Ti$ reactions for 1 h irradiation. The values are shown as curves as a function of particle energy.

Fig. 6 Excitation functions of the reactions $^{nat}Cr(p,xn)^{52}Mn$ and $^{nat}Cr(p,xn)^{51}Mn$ based on data reported in Refs. [95-100]. The curves are eye-guides.

Table 1. Positron emitters for applications [a)]

Radionuclides	Half-life	Positron decay (%) [b)]	Maximum positron energy (keV)	Average positron energy (keV)	Main γ-rays (keV) [%]
^{11}C	20.36 min	99.77	960	386	no γ
^{13}N	9.97 min	99.80	1199	492	no γ
^{15}O	2.04 min	99.90	1732	735	no γ
^{18}F	109.77 min	96.73	634	250	no γ
^{22}Na	2.602 a	90.33	546	216	1274.5 [99.9]
^{30}P	2.5 min	99.80	3210	1441	2235.2 [0.06]
^{34m}Cl	31.99 min	28.4	2488	1099	2127.5 [42.8]; 1176.7 [14.09]
		25.6	1311	554	
^{38}K	7.64 min	99.33	2724	1212	2167.5 [99.86]
^{43}Sc	3.89 h	70.9	1199	508	372.9 [22.5]
		17.2	826	345	
^{44g}Sc	3.97 h	94.27	1474	632	1157.0 [99.9]
^{45}Ti	184.8 min	$\Sigma\beta^+$ 85.7 [c)]	1040	439	719.6 [0.15]
^{48}V	15.974 d	49.9	695	290	983.5 [99.98]; 1312.1 [98.2]

^{49}Cr	42.3 min	46.4	1452	625	90.6 [53.2]; 152.9 [30.3]
		34.7	1514	653	
		11.7	1605	694	
^{51}Mn	46.2 min	97.08	2186	964	749.1 [0.265]
^{52m}Mn	21.1 min	96.4	2633	1174	1434.1 [98.2]
^{52g}Mn	5.59 d	29.4	575	242	1434.1 [100.0]; 935.5 [94.5]; 744.2 [90.0]
^{52}Fe	8.28 h	55.49	800	340	168.7 [99]
^{55}Co	17.53 h	46	1499	649	931.1 [75]; 477.2 [20.2]; 1408.5 [16.9]
		25.6	1021	436	
		4.26	1113	475	
^{56}Co	77.24 d	18.4	1459	631	846.8 [99.9]; 1238.3 [66.5]; 2598.5 [17.0]
^{58}Co	70.86 d	14.9	475	201	810.8 [99.45]
^{57}Ni	35.60 h	35.3	865	369	1377.6 [81.7]; 126.2 [16.7]; 1919.5 [12.3]
		7.0	737	314	
^{60}Cu	23.7 min	49.0	1982	872	1332.5 [88.0]; 1791.6 [45.4]; 826.4 [21.7]
		15.0	2947	1325	
		11.6	1912	840	
^{61}Cu	3.34 h	51	1982	524	283.0 [12.2]; 656.0 [10.8]
		5.5	933	399	

		2.6	560	239	
^{62}Cu (Zn)	9.67 min [f)]	97.60	2937	1321	1173.0 [0.34]
^{64}Cu	12.70 h	$\Sigma\beta^{+}$ 17.8 [d)]	653	278	1345.8 [0.54] [d)]
^{62}Zn	9.19 h	8.2	598	255	596.6 [26.0]; 548.4 [15.3]
^{63}Zn	38.47 min	80.3	2345	1042	669.6 [8.2]; 962.1 [6.5]
		7.0	1675	733	
		4.9	1382	600	
^{66}Ga	9.49 h	51	4153	1904	1039.2 [37.0]; 2751.8 [22.7]
		3.7	924	397	
^{68}Ga (Ge)	67.71 min [f)]	87.72	1899	836	1077.3 [3.2]
		1.19	822	353	
^{71}As	65.30 h	27.9	816	352	174.9 [82.4]
^{72}As	26.0 h	64.2	2500	1117	834.0 [81.0]; 629.8 [8.1]
		16.3	3334	1529	
		5.82	1870	824	
^{74}As	17.77 d	$\Sigma\beta^{+}$ 29	1541	701	595.8 [59]
^{73}Se	7.15 h	64.7	1290	562	361.2 [97.0]

^{75}Br	96.7 min	53	1753	773	286.5 [88]
		4.9	1612	708	
		4	2040	904	
^{76}Br	16.2 h	$\Sigma\beta^+$ 58.2 [d)]	3941	1800	559.1 [74.0]; 657.0 [15.9]
^{77}Kr	74.4 min	41.8	1914	907	129.6 [81.0]; 146.6 [37.3]
		33.6	1767	780	
^{82m}Rb	6.47 h	19.7	798	353	776.5 [84.4]; 554.4 [62.4]
^{82g}Rb (Sr)	1.3 min [f)]	81.8	3378	1535	776.5 [15.08]
		13.1	2601	1168	
^{83}Sr	32.41 h	$\Sigma\beta^+$ 26	1251	548	762.7 [26.7]; 381.5 [14.0]
^{86g}Y	14.74 h	$\Sigma\beta^+$ 33	1251	535	1076.6 [82.5]; 627.7 [32.6]
^{89}Zr	78.42 h	22.74	902	396	909.2[99.04]
^{94m}Tc	52.0 min	67.6	2439	1094	871.1 [94.2]
^{95}Ru	1.643 h	12.6	1207	533	336.4 [69.9]
^{110m}In	69.1 min	60.7	2260	1015	657.8 [97.74]
^{118g}Sb	3.6 min [f)]	73.2	2635	1189	1229.3 [2.5]

^{120}I	81.6 min	Σβ^{+} 56.1 [c)]	4033	1845	560.4 [69.6]
^{122}I	3.63 m [f)]	67 10	3212 2648	1458 1195	564.1 [18] 692.8 [1.4] 793.3 [1.3]
^{124}I	4.18 d	Σβ^{+} 22.1 [d)]	2138	975	602.7 [62.9]
^{138m}Pr (Nd)	2.12 h [f)]	23	1650	742	1037.8 [101]; 788.7 [100]
^{149}Tb	4.12 h	Σβ^{+} 5	1798	811	352.2 [29.4]; 165.0 [26.4]; 388.6 [18.4]
^{152}Tb	17.5 h	Σβ^{+} 18	2970	1337	344.3 [63.5]

a) Data taken mostly from ENSDF [Ref. 3], unless otherwise stated.
b) For a few radionuclides, serveral strong positron groups exist. They are separately listed. The remaining % decay is via EC, except for ^{64}Cu and ^{74}As where β^- branching of 38.4% and 32.1 %, respectively, also occurs. In case of ^{149}Tb, besides EC and β^+ emission, an α-decay branching of 16.7 % also exists.
c) S. Kuhn et al. [Ref. 4].
d) S. M. Qaim et al. [Ref. 5].
e) A. Hohn et al. [Ref. 6].
f) Short-lived generator produced.

Table 2. Common methods of production of standard positron emitters

Nuclide	T½	Production route	Energy range [MeV]	Thick target yield[a] [MBq/µAh]	Target	Target condition	In-target precursor	Typical batch yield [GBq]
^{11}C	20.4 min	$^{14}N(p,\alpha)$	13 → 4	3820	$N_2(O_2)$	(gas)	$^{11}CO_2$	> 100
^{13}N	10.0 min	$^{16}O(p,\alpha)$	16 → 7	1665	$H_2{}^{16}O$	(liquid)	$^{13}NO_3^-$	30
^{15}O	2.0 min	$^{14}N(d,n)$	8 → 0	2368	$^{14}N_2(O_2)$	(gas)	$[^{15}O]O_2$	100
		$^{15}N(p,n)$	10 → 0	2220	$^{15}N_2(O_2)$	(gas, > 99 % enriched)	$[^{15}O]O_2$	80
^{18}F	109.8 min	$^{18}O(p,n)$	16 → 3	3893	$H_2{}^{18}O$	(liquid, > 95 % enriched)	$^{18}F_{aq}^-$	150
					$^{18}O_2/(F_2)$	(gas, > 98 % enriched)	$[^{18}F]F_2$	40
		$^{20}Ne(d,\alpha)$	14 → 0	1110	$Ne(F_2)$	(gas)	$[^{18}F]F_2$	25
^{22}Na	2.6 a	$^{nat}Mg(d,x)$	26 → 5	0.19	Mg or Mg_2Cu	(solid)	Na^+	0.15
		$^{nat}Mg(p,x)$	61 → 40	1.0	Mg	(solid)	Na^+	11
		$^{27}Al(p,x)$	70 → 25	0.54	Al	(solid)	Na^+	1.3
^{68}Ga	1.1 h	$^{nat}Ga(p,xn)^{68}Ge$	70 → 20	2.5	$^{nat}Ga_2O_3$	(solid)	$^{68}Ge \rightarrow {}^{68}Ga$ (generator)	40
^{82}Rb	1.3 min	$^{nat}Rb(p,xn)^{82}Sr$	70 → 50	9.2	$^{nat}RbCl$	(solid)	$^{82}Sr \rightarrow {}^{82}Rb$ (generator)	70

[a] Calculated from the respective excitation function [cf. 27], assuming 100 % enrichment of the target isotope for an irradiation time of 1 h, except for ^{18}F via the $^{18}O(p,n)^{18}F$ reaction where the data by Hess et al. [28] were used. For calculation of ^{22}Na yields, average cross sections given in EXFOR were used (see text).

Table 3. Methods of production of some non-standard positron emitters for medical applications [a)]

Nuclide	**Half-live**	**Major production route**	**Energy range [MeV]**	**Thick target yield [MBq/μAh]** [b)]	**Application**
^{44g}**Sc**	3.9 h	^{44}Ca(p,n)	18 → 6	2300	Therapy planning
^{45}**Ti**	3.1 h	^{45}Sc(p,n)	14.5 → 5	433	Tumour imaging
^{52g}**Mn**	5.6 d	^{nat}Cr(p,x)	17 → 8	14	Multimodal imaging, (PET + MRI)
^{52}**Fe**	8.3 h	^{55}Mn(p,4n)	100 → 60	22	PET + MRI
^{55}**Co**	17.6 h	^{58}Ni(p,α) ^{54}Fe(d,n)	15 → 7 10 → 5	14 33	Tumour imaging; neuronal Ca marker
^{61}**Cu**	3.3 h	^{64}Zn(p,α)	18 → 11	288	Tumour imaging
^{64}**Cu**	12.7 h	^{64}Ni(p,n)	12 → 8	304	Radioimmunotherapy
^{66}**Ga**	9.4 h	^{66}Zn(p,n)	15 → 7	700	Quantification of SPECT
^{72}**As**	26.0 h	^{nat}Ge(p,xn)	18 → 8	114	Tumour localisation; immuno-PET
^{73}**Se**	7.1 h	^{75}As(p,3n)	40 → 30	1300	Selenopharmaceuticals
^{76}**Br**	16.0 h	^{76}Se(p,n)	15 → 7	402	Radioimmunotherapy
^{82m}**Rb**	6.2 h	^{82}Kr(p,n)	14.5 → 10	370	Cardiology
^{86}**Y**	14.7 h	^{86}Sr(p,n)	14 → 7	371	Therapy planning
^{89}**Zr**	78.4 h	^{89}Y(p,n)	14 → 9	58	Immuno-PET
^{94m}**Tc**	52 min	^{94}Mo(p,n)	13 → 7	2000	Quantification of SPECT

^{120}I	1.3 h	^{120}Te(p,n)	$15 \rightarrow 9$	2000	Iodopharmaceuticals
^{124}I	4.2 d	^{124}Te(p,n)	$12 \rightarrow 8$	16	Tumour targeting; dosimetry

a) Adapted partly from Qaim [2].

b) Calculated from the respective excitation function, assuming 100 % enrichment of the target isotope for an irradiation time of 1 h.

Figure 1

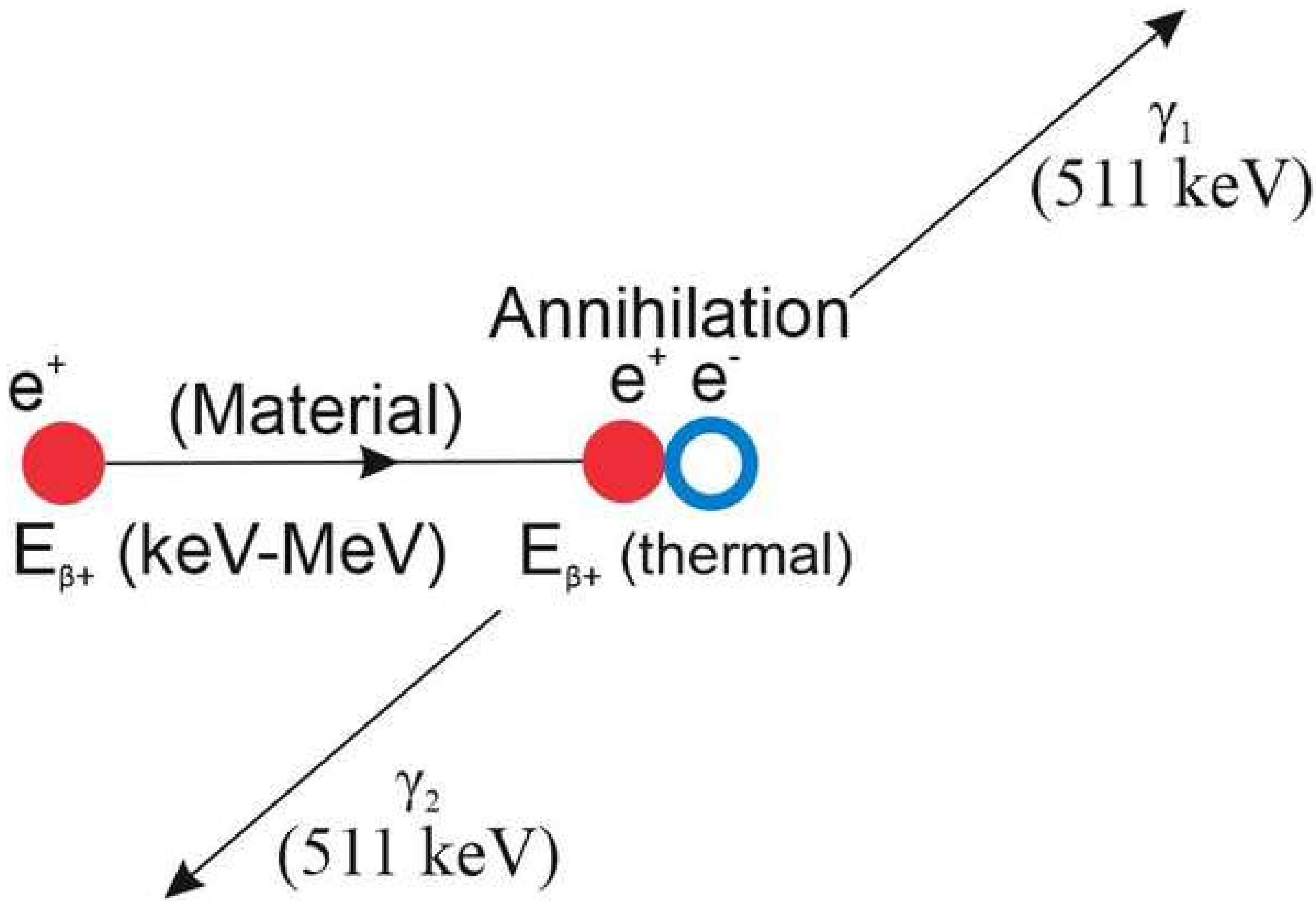
γ_1
(511 keV)
Annihilation
e^+
(Material)
e^+ e^-
$E_{\beta+}$ (keV-MeV)
$E_{\beta+}$ (thermal)
γ_2
(511 keV)

Figure 2

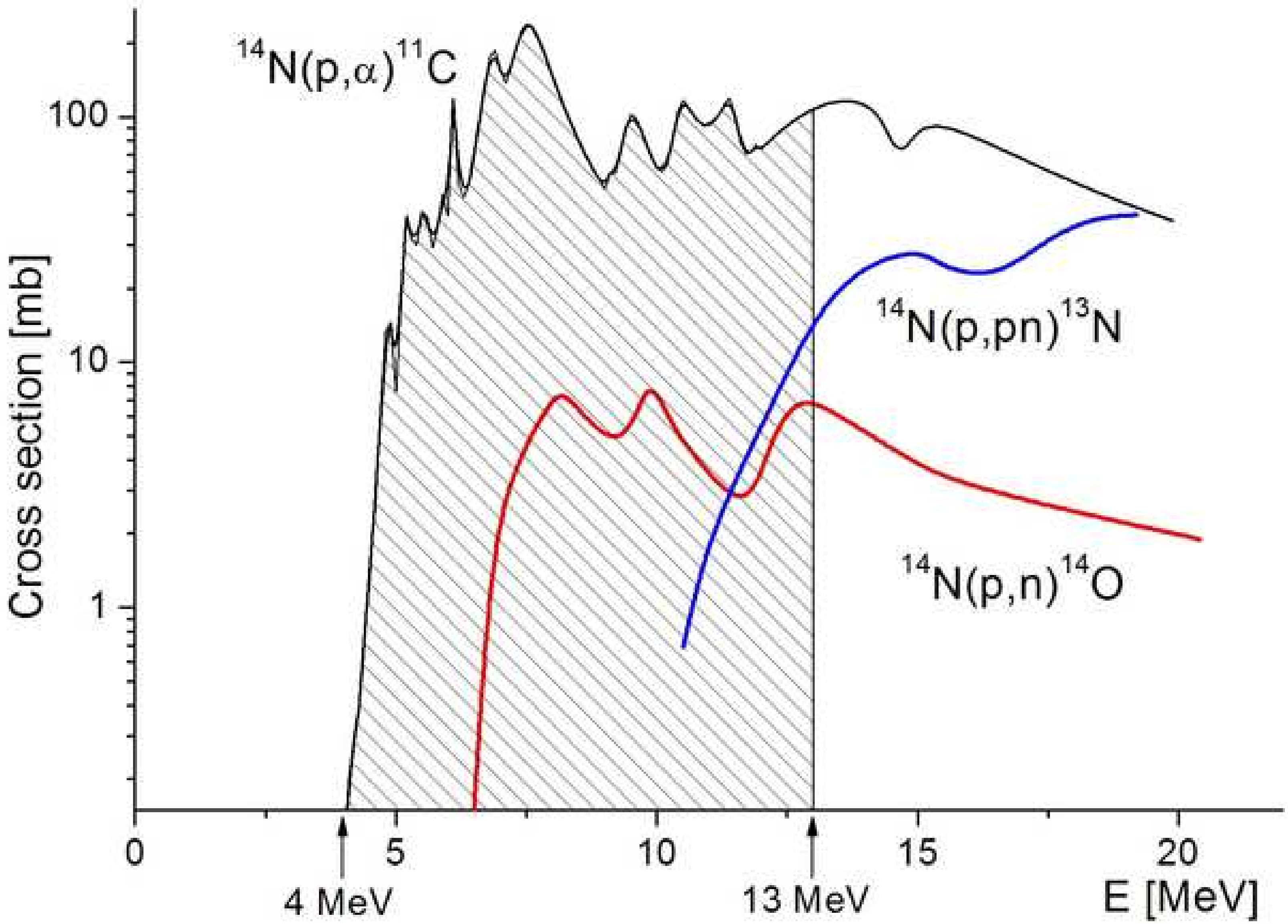
$^{14}N(p,\alpha)^{11}C$
$^{14}N(p,pn)^{13}N$
$^{14}N(p,n)^{14}O$
Cross section [mb]
100
10
1
0
5
10
15
20
4 MeV
13 MeV
E [MeV]

Figure 3a

Click here to access/download;Figure (only eps, tif, png);Fig 3a.eps

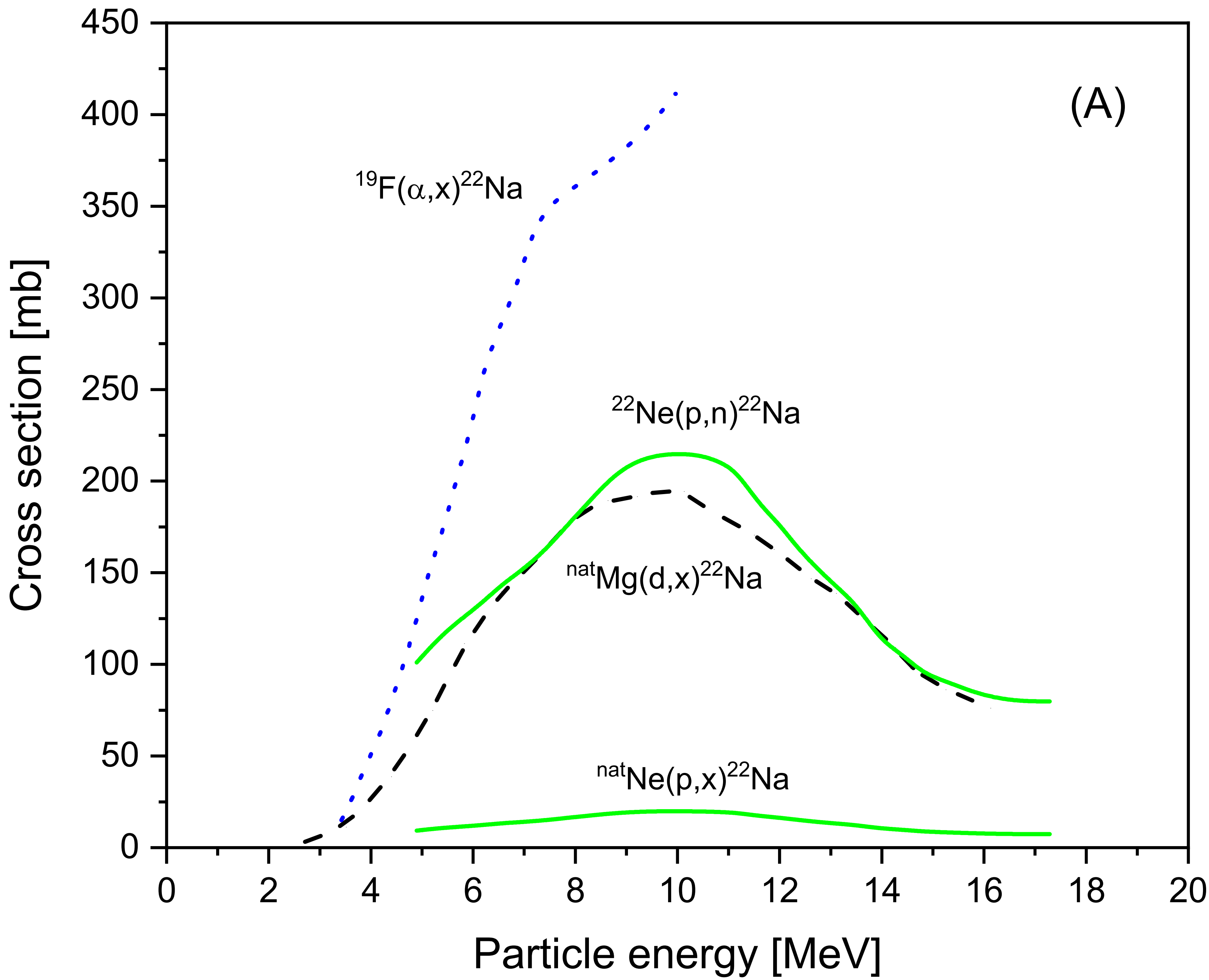

Figure 3b

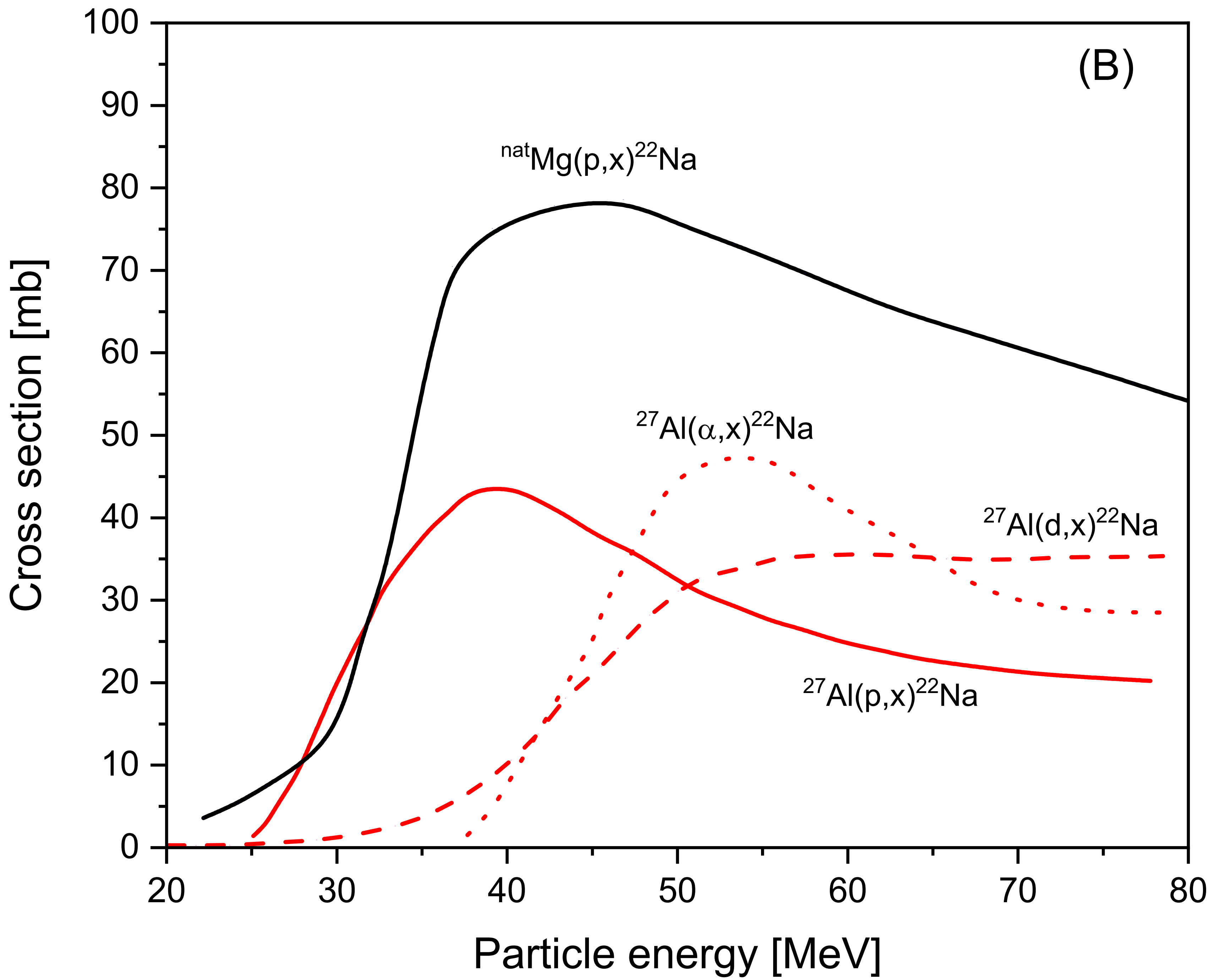
(B)
natMg(p,x)22Na
27Al(α,x)22Na
27Al(d,x)22Na
27Al(p,x)22Na
Cross section [mb]
Particle energy [MeV]
0
10
20
30
40
50
60
70
80
90
100
20
30
40
50
60
70
80

Figure 4

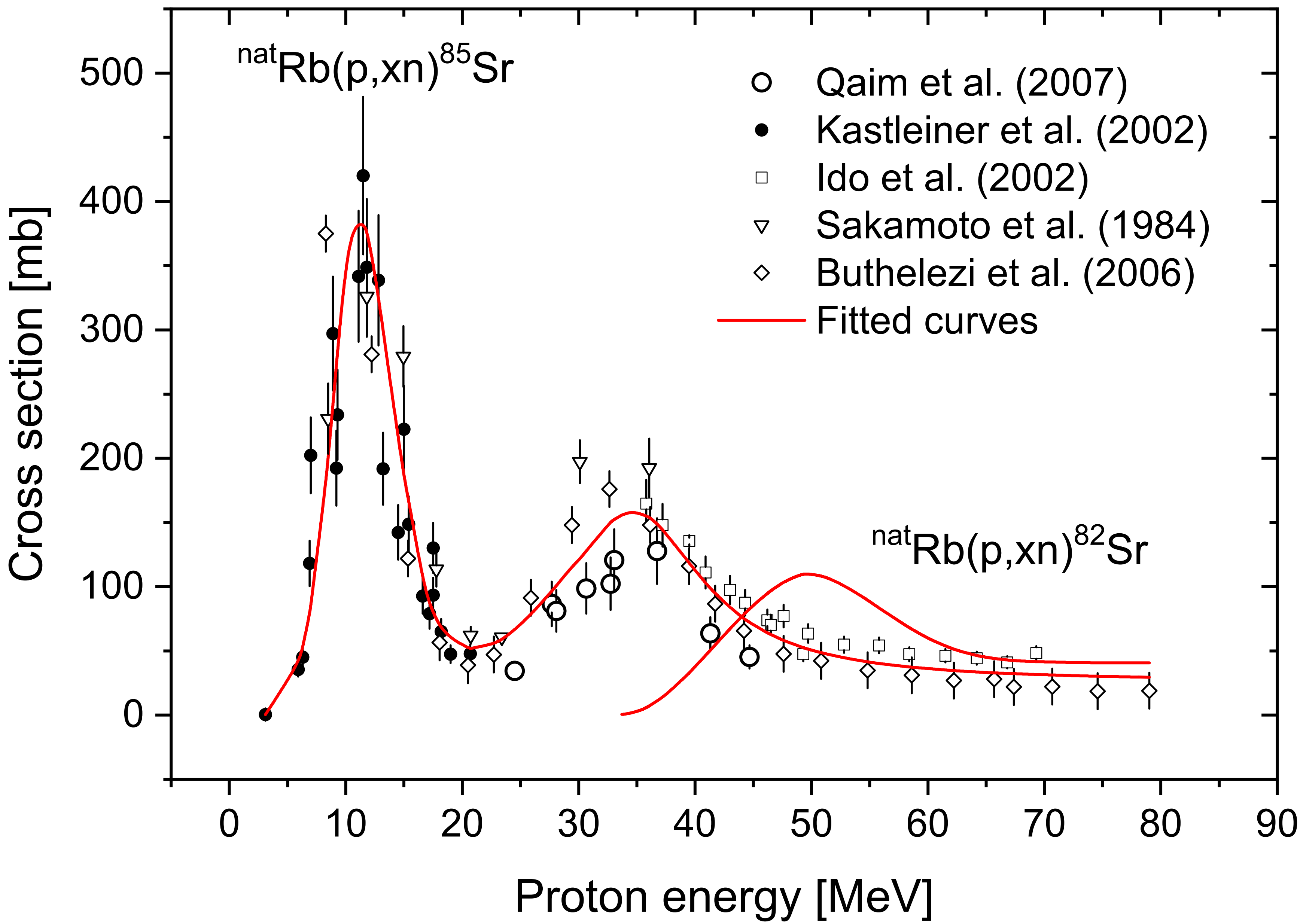

natRb(p,xn)85Sr
natRb(p,xn)82Sr
Qaim et al. (2007)
Kastleiner et al. (2002)
Ido et al. (2002)
Sakamoto et al. (1984)
Buthelezi et al. (2006)
Fitted curves
Cross section [mb]
Proton energy [MeV]
500
400
300
200
100
0
0
10
20
30
40
50
60
70
80
90

Figure 5

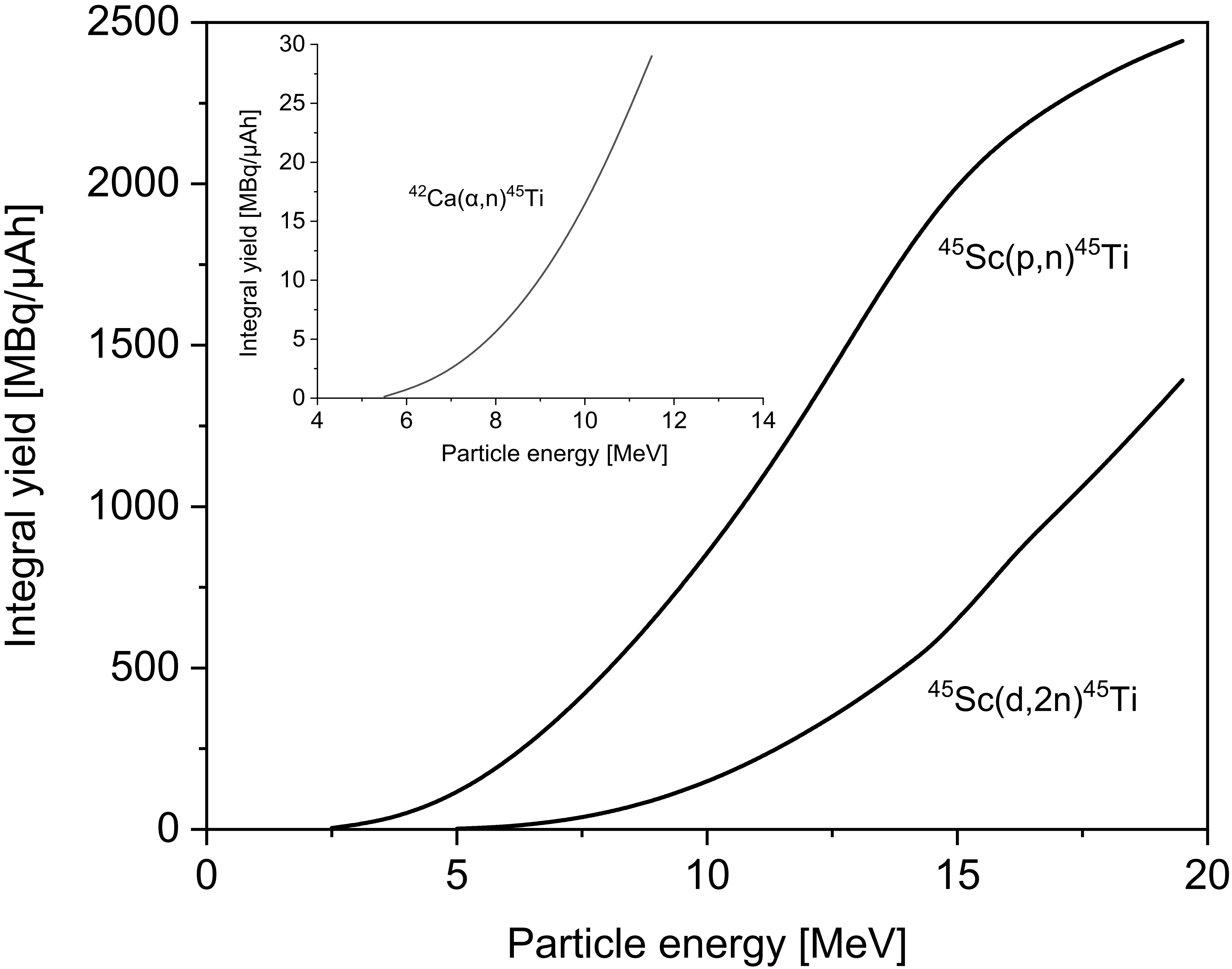

2500
2000
1500
1000
500
0
0
5
10
15
20
Integral yield [MBq/μAh]
Particle energy [MeV]
45Sc(p,n)45Ti
45Sc(d,2n)45Ti
30
25
20
15
10
5
0
4
6
8
10
12
14
Integral yield [MBq/μAh]
Particle energy [MeV]
42Ca(α,n)45Ti

Figure 6

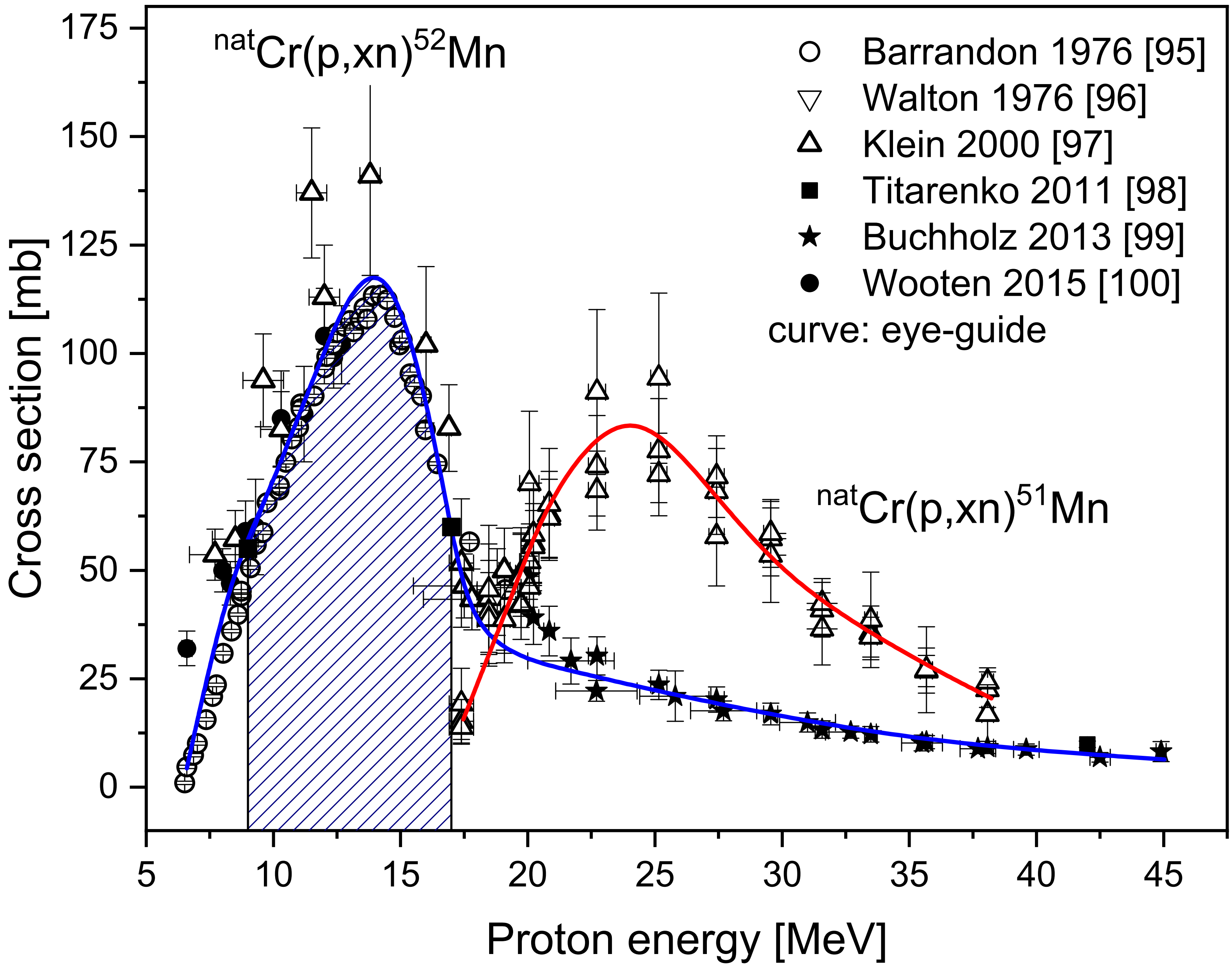

natCr(p,xn)52Mn
natCr(p,xn)51Mn
Barrandon 1976 [95]
Walton 1976 [96]
Klein 2000 [97]
Titarenko 2011 [98]
Buchholz 2013 [99]
Wooten 2015 [100]
curve: eye-guide
Cross section [mb]
Proton energy [MeV]
0
25
50
75
100
125
150
175
5
10
15
20
25
30
35
40
45